Multi-scale nitrate transport in a sandstone aquifer system under intensive agriculture

Daniel Paradis[1], Jean-Marc Ballard[2], René Lefebvre[2] and Martine M. Savard[1]

1: Geological Survey of Canada, 490 rue de la Couronne, Quebec City, Canada G1K 9A9

2: Institut national de la recherche scientifique, Centre Eau Terre Environnement (INRS-ETE), 490 rue de la Couronne, Quebec City, Canada G1K 9A9

Corresponding author: Daniel Paradis

Phone: (418) 654-3713   Fax: (418) 654-2604   E-mail: daniel.paradis@canada.ca

KEYWORDS: Nitrate; Numerical modeling; Sandstone; Canada

ABSTRACT

Nitrate transport in heterogeneous bedrock aquifers is influenced by mechanisms that operate at different spatial and temporal scales. To understand these mechanisms in a fractured sandstone aquifer with high porosity, a groundwater-flow and nitrate transport model – reproducing multiple hydraulic and chemical targets – was developed to explain the actual nitrate contamination observed in groundwater and surface water in a study area on Prince Edward Island, Canada. Simulations show that nitrate is leached to the aquifer year-round, with 61% coming from untransformed and transformed organic sources originating from fertilizers and manure. This nitrate reaches the more permeable shallow aquifer through fractures in weathered sandstone that represent only 1% of the total porosity (17%). Some of the nitrate reaches the underlying aquifer, which is less active in terms of groundwater flow, but most of it is drained to the main river. The river water quality is controlled by the nitrate input from the shallow aquifer. Groundwater in the underlying aquifer, which has long residence times, is also largely influenced by the diffusion of nitrate in the porous sandstone matrix. Consequently, following a change of fertilizer application practices, water quality in domestic wells and the river would change rapidly due to the level of nitrate found in fractures, but a lag time of up to 20 years would be necessary to reach a steady level due to diffusion. This demonstrates the importance of understanding nitrate transport mechanisms when designing effective agricultural and water management plans to improve water quality.

1 Introduction

Worldwide, the need to meet increasing food production demand is pushing the agriculture industry to use increasing amounts of nitrogen-enriched fertilizers. Under such circumstances, one of the most important environmental challenges is to prevent nitrate from contaminating groundwater, which is the safest source of drinking water for many rural communities (WHO, 2007). From an agronomic perspective, the protection of groundwater involves minimizing excess nitrogen (N) in the root zone to reduce the risks of nitrate transformation to N and nitrate leaching to the aquifer (Keeney and Follett, 1991). This protection is generally implemented through best management practices (BMP), aiming at changing agricultural practices to limit the contamination risks to water in sensitive receivers (e.g., rivers, aquifers). The success of such BMPs depends essentially on the kind of local agricultural methods (e.g., crops grown, crop rotation and fertilizer application) that define the amount of N available to leaching; and site-specific physical factors (e.g., climate, soil and geology) that control the transport of pollutants from the fields to the sensitive receivers. Then, understanding the factors controlling nitrate transformation and transport in their local contexts is essential to the design of effective BMPs (Laurent and Ruelland, 2011).

Several experimental studies at the plot scale have investigated the sensitivity of various parameters (e.g., climate, soil, crops, farming practices) on the efficiency of BMPs aimed at reducing nitrate leaching (e.g., Blombäck et al., 2003; Beaudoin et al., 2005; Constantin et al., 2010). In these studies, parameters are varied and the amount of nitrate leached below the root zone is monitored and modelled to assess the impact in term of groundwater nitrate contamination. The transferability of small-scale results at watershed scale is however rather limited. Distributed physically-based hydrological models are thus commonly used for a more comprehensive understanding of nitrate contamination at the watershed scale (e.g., Vaché et al., 2002; Hattermann et al., 2005; Bracmort et al., 2006; Rode et al., 2009). The representation of aquifers in hydrological models is generally over-simplified, with flow and transport processes modelled through simple transfer functions, which for complex aquifer systems may not be adequate to simulate the spatial and temporal distribution of nitrate contamination in groundwater and its transport to downstream surface-water receivers. For this key task, understanding aquifer dynamics, especially groundwater residence times, is crucial to support agricultural and water management plans, given that the contamination intensity and time needed for water quality to change as a result of BMPs both depend to a great extent on hydrogeological characteristics. Therefore, many researchers have taken into account the dynamics of aquifers using numerical groundwater models (e.g., Lunn et al., 1996; Vinten and Dunn, 2001; Molénat et al., 2002; Wriedt and Rode, 2006; Dimitriou et al., 2010; Paradis et al., 2016). Numerical modeling of groundwater flow and nitrate transport in aquifers can provide quantitative insight into water quality sustainability as long as model parameters (e.g., hydraulic property values and structures) and inputs (e.g., groundwater recharge, nitrate flux) are reasonably well established (Michael and Voss 2009). Estimation of model parameters and inputs can be difficult, notably for large aquifers with limited data. To narrow the range of model uncertainties, model calibration with multiple data sets is generally proposed, with each data set providing different and complementary constraints on the aquifer model (e.g., Kim et al., 1999).

In this paper, the control exerted by the dynamics of a sandstone aquifer on groundwater contamination by nitrate, in a watershed with intensive agriculture, is examined using a groundwater flow and nitrate transport model. The heterogeneous and dual-porosity nature of the aquifer revealed by field and laboratory data were expected to influence water quality, but the magnitude and trends of the contamination still remained unknown. To address this shortcoming, the nitrate transport mechanisms within the aquifer were inferred from the groundwater flow and nitrate transport model using calibrated aquifer parameters on the basis of various types of monitoring data, such as water levels, nitrate concentrations in groundwater and surface water, and nitrate isotopic values ($\delta^{15}N$ and $\delta^{18}O$) in groundwater. Using this model, the study objectives are thus to: (i) better understand the dynamics of nitrate input and leaching through the unsaturated zone into the groundwater saturated system, (ii) reproduce the historical evolution in time and space of nitrate contamination in groundwater, and (iii) assess the potential future evolution of nitrate contamination considering scenarios of nitrate leaching to the aquifer associated with different agro-economic contexts.

2 General methodology

2.1 Study area

The Wilmot watershed is located in west central Prince Edward Island (PEI), Canada (Figure 1). The Wilmot River drains an area of about 87 km^2 and flows southwesterly to Bedeque Bay with watershed dimensions of approximately 17 km long by 5 km wide (Table 1). Half of the river is tidally influenced and its elevation ranges from sea level in the tidal area, to 90 m in the headwater area. Streamflow data for the Wilmot River collected above the tidally influenced area show a mean annual discharge of 0.92 m^3/s (Station 01CB004 in Figure 1; 1972-1999) and a mean monthly discharge ranging from 0.45 m^3/s in September to 1.88 m^3/s in April, during the spring freshet (Table 1). The climate of the island is humid-continental, with long, fairly cold winters and warm summers. Mean annual precipitation is 1078 mm (Station Summerside A in Figure 1; 1971 to 2000), most of which falls as rain (75%) (Table 2). The mean annual temperature is 5.1°C and monthly mean temperatures range from -8.6°C in January to 18.4°C in July (Table 2).

The Wilmot watershed area is almost entirely covered by glacial material defined as permeable unconsolidated sandy tills, a few centimeters to several meters thick (Prest, 1973). That layer is underlain mostly (80-85%) by fine to medium-grained fractured sandstone, with some siltstone and claystone forming isolated lenses (Van de Poll, 1983). The sandstone is a fractured porous medium characterized by a well-developed network of fractures and a high porosity matrix (17% on average for sandstone according to Francis, 1989). Groundwater is the only source of fresh water on PEI and most of the drinking water comes from domestic wells withdrawing groundwater from the sandstone aquifer. The water table of this unconfined aquifer is mostly shallow, which results in an unsaturated zone of only a few meters. Analysis of groundwater levels and river stages also suggests that the Wilmot River receives an important amount of groundwater from the sandstone aquifer most of the year.

The Wilmot watershed is predominantly rural with less than 10% of its surface dedicated to residential uses and agricultural activities covering as much as 76% of the watershed (Figure 1 and Table 1). Potato production is the most important agricultural activity in the watershed. Almost 80% of the agriculture is involved in a potato crop rotation with grain and hay for forage. At the time of the field study, a summary of agricultural practices showed that since 2002, 33% of cropland was in a two-year crop rotation, 33% was in a three-year crop rotation (1 y grain, 1 y hay, 1 y potato) and 33% was in a two-in-five-year rotation (AAT, 2006). In many areas of the PEI, and in particular in the Wilmot watershed, nitrate concentrations in drinking water coming from groundwater sources exceed background levels and, in some cases, the Health Canada (2004) recommended maximum concentration of 10 mg/L (*N-NO_3*) for drinking water (Somers, 1998; Somers et al., 1999). In addition to being a concern for drinking water quality, excessive nitrate levels contribute to eutrophication of surface waters, especially in estuarine environments (Somers et al., 1999). Several studies that have documented the nitrate problem in PEI groundwater suggest that elevated nitrate levels are often associated with agricultural activities, especially the use of fertilizers for row crop production (Somers, 1992; Somers, 1998; Somers et al., 1999; Young et al., 2003; Benson et al., 2006; Savard and Somers, 2007; Paradis et al., 2016). Furthermore, the census of agriculture for PEI has shown that agricultural activities had increased by more than 15% over 25 years from approximately 1980, mainly due to an increase by 80% of potato acreage (AAFC, 2004), which may explain the historical trend toward increasing nitrate levels noted in surface water and groundwater (Somers et al., 1999). Thus, a comprehensive understanding of the nitrate problem is needed to propose effective solutions tailored to the specific context of PEI: vulnerable aquifer, total dependence on groundwater, strong relationship of rivers to groundwater, and widespread agricultural activities having a vital economic role.

Figure 1

Table 1

Table 2

2.2 Hydrogeological characteristics of the Wilmot aquifer

The sandstone aquifer in the Wilmot Watershed is both fractured and porous, which leads to drastically different ranges of values for total porosity (n), effective porosity, and specific yield S_y

(the drainable part of "effective" porosity). Fractures control the hydraulic conductivity and groundwater flow whereas the low hydraulic conductivity of the porous sandstone matrix does not allow significant flow. The effective porosity through which flow occurs will thus correspond to the low fracture porosity. However, the significant (non-effective) porosity of the matrix contributes to groundwater storage and impacts mass transport, as mass transported with groundwater flow in the fractures (such as nitrates) will diffuse in the porous matrix (Pankow and Cherry, 1996). On the contrary, fractures only account for a small proportion of the *n* of the aquifer, so the matrix porosity of the sandstone can be considered almost equivalent to the *n* of the aquifer. However, the low hydraulic conductivity and large capillary retention capacity of the sandstone matrix implies that the matrix will not drain when the water table fluctuates seasonally during recharge periods. Drainage and infiltration near the water table will rather occur almost exclusively in fractures, who will thus control the S_y (drainage of effective porosity) of the aquifer. The S_y of the aquifer will thus be quite low, corresponding to only part of the porosity of fractures, the porous matrix remaining saturated.

For the purpose of this study, a numerical groundwater flow and mass transport model was developed using FEFLOW, a proven simulator using finite elements (Diersch, 2004). To support the numerical model development, field work was carried out to evaluate the hydrogeological characteristics of the aquifer. The hydrogeological properties were mainly determined using three sets of three nested piezometers installed along a transverse section through the watershed (monitoring sites WIL-1, WIL-2 and WIL-3 are shown in Figure 1). The piezometers reach depths between 1 and 85 m below the water table. Before boreholes were converted to piezometers, profiles of horizontal hydraulic conductivity (K_h), hydraulic heads, nitrate concentrations and groundwater ages were obtained at WIL-2 and WIL-3 by isolating discrete intervals of the open boreholes with a dual-packer system straddling a 6 m screen. Within each interval, static water levels were recorded, slug tests were carried out to estimates K_h and groundwater samples were collected with a submersible pump. Results of this field work and comparison with previous analyses in the study area form the conceptual model of the Wilmot aquifer as briefly described below.

Firstly, the hydraulic head and K_h profiles for boreholes WIL-2 and WIL-3, shown in Figure 2, indicate that the sandstone aquifer comprises a high flow (HF) and a low flow (LF) interval. The HF interval ranges from the water table to a depth of 18 to 36 m, whereas the LF interval extends below the HF interval. K_h in the HF interval is relatively higher than in the LF interval with average values for the tested wells of 1.3x10^{-4} m s^{-1} and 3.5x10^{-5} m s^{-1}, respectively. The higher K_h for the HF interval is likely the results of more important weathering processes and less overburden pressure resulting in increased fracture aperture and frequency. Similar profiles were obtained by Francis (1989) in the Winter River watershed of PEI, which is about 50 km from the Wilmot watershed. Also, the vertical hydraulic conductivity (K_v), estimated from K_h profiles using the geometric mean of K_h (e.g., Freeze and Cherry, 1979), shows a moderate K_v/K_h ratio (K anisotropy) that varies by 1 to 2 orders of magnitude due to alternating high and low K_h layers. However, slug testing over a 6 m long screen may not capture all the vertical K_h variability and these ratios should be considered as minimum values for the purpose of calibrating the numerical model (e.g., Paradis and Lefebvre, 2013). In addition, K_h estimates from 23 slug tests in the sandstone aquifer range from 9x10^{-7} to 4x10^{-4} m s^{-1} while those obtained with a laboratory Bernaix type permeameter on undisturbed (without fractures) cores range from 1x10^{-8} to 5x10^{-7} m s^{-1} for sandstone and as low as $5x10^{-10}$ m s^{-1} for mudstone (Francis, 1989). Comparison between field and laboratory estimates suggests thus that fractures play an important role in the bulk rock permeability. Cores reveal that horizontal bedding of the sandstone forms the main fracture network above 35 m depth with 82% of all fractures (Francis, 1989). At a larger scale, the weathered HF interval generally provides a typical porous media response to pumping, which suggests a relative homogeneity of the distribution and interconnection of the fractures.

Secondly, n measurements on undisturbed cores by Francis (1989) show values averaging 17% for the sandstone aquifer. The comparison of the low K_h values for undisturbed cores representing sandstone matrix relative to the much higher values for fractured sandstone suggests that the contribution of the porous matrix to groundwater flow is insignificant. Accordingly, the S_y of the sandstone can be attributed entirely to the fractures that are the only part of the fractured porous medium that seasonally drain. While storage of nitrate in the matrix is possible through advection with dissolved nitrate in the water, diffusion of nitrate between the fractures and the matrix is also likely to occur. Use of the analytical solution of Mutch and Scott (1993), which takes into account diffusion from the fractures to the matrix, reveals that 70% of the sandstone matrix contains nitrate after only 2 to 3 years of contact with nitrate in fractures, and the matrix is full after 10 years. This estimate is based on an average distance between fractures of 0.25 m and an effective diffusion coefficient of $9.8x10^{-11}$ m^2 s^{-1} based on the Millington and Quirk (1961) relationship for a temperature of 5 °C. Thus, there is a relatively rapid transfer of nitrate from fractures to the sandstone matrix through diffusion. Then, the sandstone aquifer represents a double porosity system with permeable fractures providing groundwater flow paths and the low-permeability porous matrix providing storage capacity for nitrate through diffusion.

Thirdly, analysis of groundwater level and precipitation records reveals that the lag time between water table fluctuations resulting from infiltrated precipitation through the unsaturated zone is only a few days (Paradis et al., 2006). This rapid infiltration is due to the large drainage capacity of the soil (<2 m in thickness), mostly composed of loamy sand with 50-65% of sand, and the high permeability of the heavily weathered sandstone (<7 m of unsaturated thickness). Thus, it is expected that much of the nitrate dissolved in water is reaching the water table by advection, and a very low proportion of this nitrate is stored by diffusion in the soil residual water and sandstone matrix. This is also supported by the preservation of seasonally distinct nitrate oxygen isotope characteristics in the groundwater of the Wilmot aquifer (Savard et al., 2007). On the other hand, the piezometric map of the sandstone aquifer shows that the water table follows the topographic relief, with the Wilmot River acting as a groundwater discharge zone (Paradis et al., 2006). This map, based on 243 domestic wells with an average saturated depth of 19 m, is thought to be representative of the HF interval. Also, analysis of streamflow records of the Wilmot River using the hydrograph separation method of Furey and Gupta (2001) shows that the groundwater contribution to the river (baseflow) accounts for 63% of the mean annual streamflow, and that baseflow may be the only source of water to the river during dry summer periods. Moreover, seasonal sampling of water for nitrate, carried out over a period of two years (2003-2005) in domestic wells (107 samples) and in the Wilmot River (17 samples), shows similar average nitrate concentration as well as water and nitrate isotopic properties (Savard et al., 2010). These observations indicate a strong hydraulic connection between the aquifer and the river.

Finally, analyses on groundwater samples in the HF interval at WIL-3 indicate the presence of tritium (enriched tritium analysis method), which is an indication of the presence of young groundwater recharged less than 50 years ago. Also, hydrogen and oxygen isotopes for groundwater sampled in domestic wells open to the HF interval fall on or near the meteoric water line for the region, indicating that groundwater is likely derived entirely from modern local precipitation (Liao et al., 2005). In the LF interval, no tritium is observed but corrected carbon-14 (^{14}C) analyses (of dissolved inorganic carbon) for carbonates dissolution (e.g., Clark and Fritz, 1997) provide groundwater age between 2 000 and 3 000 years at depths between 50 and 85 m below the water table. Thus, besides hydraulic data, there is strong isotopic evidence for an aquifer system having two intervals (HF and LF) with significantly different magnitudes of groundwater flow. Also, as nitrate denitrification is unlikely to occur in the aquifer due to the prevailing oxidizing conditions and that no natural geological sources of nitrate are known, nitrate concentration in groundwater is mainly controlled by groundwater recharge leaching to the aquifer the available mass of nitrate in the soil.

2.3 Nitrate sources in groundwater from isotopes

Nitrate $\delta^{15}N$ and $\delta^{18}O$ analyses were carried out by Savard et al. (2007) to quantify the relative proportions of the different nitrate sources present in groundwater throughout a year. Total nitrate concentration and isotope ratios in groundwater were obtained over the entire watershed from 16 domestic wells sampled between June 2003 and May 2005 for 8 consecutive seasons (Figure 1). To derive the proportions of nitrate sources, a geochemical mixing model using the average seasonal nitrate isotope values was developed. Results of this analysis provide the following indications (Figure 3):

- Total nitrate concentrations ranged from undetected to 14.6 mg/L, with an average of 6.9 mg L^{-1} and a standard-deviation of 4.6 mg L^{-1} for the 2-year period. The high variability of nitrate concentrations between wells, without a spatial trend, is controlled by variations in land use, field conditions and well locations and installations. However, seasonal average nitrate concentration shows a narrow range of variation between 5.5 mg L^{-1}, in the spring time of the 1st year, to 8.1 mg L^{-1}, in the summer of the 2nd year.
- Although seasonal total nitrate concentration remains fairly steady, there is seasonal variability in the proportions of the three nitrate sources making up this concentration: chemical fertilizers and manure have higher proportions during summer (respectively about 50% and 20%), whereas soil organic matter (SOM) is the main source of nitrate in winter and spring. Note that the three nitrate sources represent 95% of the total nitrate concentration; the remaining 5% coming from assumed constant direct atmospheric deposition.

From an agronomic standpoint, high proportions of chemical fertilizers in summer and fall agree with a unique late spring to mid-summer application at the start of growing seasons (Somers et al., 2007). For manure, this single high proportion season is in contradiction with the two known periods of application, one in late spring or early summer and one in the fall. The proportion from soil organic matter is above 30% all year. This suggests that bacterial nitrification occurs before nitrate leaching, even in winter, such as suggested by Savard et al. (2010) for the study area and further discussed in Section *Groundwater nitrate transfer to river and distribution within the aquifer*.

Figure 3

2.4 Description of the numerical models

For this study, the dynamics of the Wilmot watershed aquifer was modelled using the numerical simulator FEFLOW. FEFLOW is a physically-based computer program for simulating groundwater flow and mass transfer in porous media and fractured media (Diersch, 2004). The program uses the finite elements numerical method to solve the three-dimensional groundwater flow equation of both saturated and unsaturated conditions as well as mass transport. FEFLOW's validity has been checked for a wide range of problems and geological contexts (e.g., Cui et al., 2010; 2012). This simulator has been selected for this research because it can also simulate non-point source nitrate contamination using inputs of groundwater recharge and nitrate flux reaching the aquifer.

2.4.1 Model discretization, hydraulic parameters and boundary conditions

For this study, two complementary numerical models were developed. First, a deep model encompassing all the intervals of the Wilmot aquifer was developed to assess the long-term effects of nitrate transport mechanisms on nitrate distribution and future evolution within the system. This model was also used to reconstruct historical nitrate flux. Then, a shallower version of this model with only the uppermost section of the HF interval was used to identify the main nitrate transport mechanisms over shorter time frames through simulation of modified nitrate source inputs. This model also provided insights about seasonal nitrate transformation.

The deep model was divided into three main zones according to the previous conceptual model (Table 3). First, the HF interval is characterized by higher K_h, especially in its uppermost part, with a strong decrease in values with depth. These changes in hydraulic conductivities with depth are meant to reflect an inferred decrease in fracturing with increasing depth. This zone was then subdivided into four layers to better represent this vertical trend in K_h. The thickness of each layer was fixed (5 to 10 m), except for the first layer whose thickness was allowed to adapt to the position of the water table. Then, the shallow LF interval, which is a less active interval than the HF interval with lower K_h, was subdivided in two layers of 25 and 50 m, respectively. Finally, the deep LF interval, which is the very deep aquifer interval with quasi-static groundwater due to the very low K_h, was subdivided in two layers of 100 m each. Considering the very rapid infiltration of water and dissolved nitrate through the unsaturated soil and weathered sandstone, the unsaturated zone was not explicitly represented in the model. However, unconfined conditions were simulated for the top layer using the movable mesh feature available in FEFLOW. This technique represents the elevation of the water table surface by vertically moving the specified top layers of the numerical grid so that the top surface of the grid is exactly positioned at the water table elevation. To use this movable mesh feature of FEFLOW, S_y values have to be specified for the layers that are allowed to move in order to represent their associated drainage. The resulting three-dimensional numerical grid contained 72,088 six-node triangular elements with an average area of 11,114 m^2 (≈150 m x 150 m).

The K_h values for the first five layers were initially estimated from field testing, whereas values for layers 6 to 8 were based on literature (Domenico and Schwartz, 1998) and from permeability tests on undisturbed rock cores. Hydraulic conductivity anisotropy (K_v/K_h) for each model layer was mainly based on the K_h profiles and the fracture analysis of Francis (1989). As conceptualized, the top of the HF interval (layer 1) and the deep LF interval (layers 7 and 8) can be considered isotropic (K_v/K_h close to 1). The former is due to the highly fractured conditions of the sandstone, while the latter is due to the absence of fractures in unaltered sandstone. The bottom of the HF interval and the shallow LF interval (layers 3 and 6) have the highest anisotropy (lower K_v/K_h) due to the presence of scattered fractures. Those values of K_h and K_v/K_h were then further adjusted during the calibration (Table 3).

For all simulations, an equivalent porous medium was assumed using different storage properties according to the conditions and scales (temporal and spatial) considered for transient flow and transport simulations in FEFLOW. Since fractures were not explicitly modeled, it implies that an instantaneous diffusion of nitrate between the actual fractures and matrix of the aquifer is assumed. This assumption is justified by the facts that the matrix does not contribute significantly to groundwater flow, and also by the rapid transfer of nitrate from the fractures to the matrix by diffusion (see Section *Hydrogeological characteristics of the Wilmot aquifer*). For the modelling of scenarios representing long-term nitrate leaching and transport at the watershed scale (see Section *Calibration of local-scale seasonal fluxes from nitrate sources*), a fixed n value of 17% corresponding to laboratory measurements of the sandstone matrix was used for all layers to simulate long-term transient nitrate transport as nitrate is present in the entire porous medium. Note that S_y was not specified for those simulations because although transport is transient, it was assumed to occur under steady-state groundwater flow conditions. For the simulation of the seasonal sources of nitrate at the local scale with transient conditions for both flow and transport (see Section *Simulation of flux from nitrate sources*) both S_y and n were defined through calibration. In this case the rapid infiltration of nitrate is inferred to take place mostly through fractures so the values of S_y and n are those of the fracture network. Note that no attempt was made to calibrate specific storage values of deep layers as this parameter was not sensitive to the calibration targets used.

Boundary conditions used for the model were no-flow and constant head conditions. First, because the groundwater divides of the piezometric map of the sandstone aquifer coincide with the watershed limits (Paradis et al., 2006), the outer boundaries of all layers of the model were imposed as no-flow conditions at locations corresponding to the watershed limits (Figure 1). Also, the main stem of the Wilmot River, including the Bedeque Bay outlet, were set as constant head boundaries with values corresponding to the elevations of the surface water courses. Heads were thus imposed in layer 1 for the Wilmot River, and in layers 1 and 2 for the Bedeque Bay. Imposing constant heads that way is meant to represent the hydraulic connection between the river and the aquifer.

To reduce the computational burden related of the transient simulations, a modified version of the deep numerical model was used, which represents only the uppermost part of the aquifer corresponding to the thickness of the aquifer penetrated by domestic wells. The same areal mesh size was used for both models. The trend in K with depth for the modeled sub-domain was further refined to better simulate the observed vertical trend in isotopic ratios (Table 4). Finally, as the diffusion processes occurring between the fractures and the sandstone matrix are not necessarily at equilibrium at the time scale considered for the simulations, the fraction of n that plays a role in the nitrate isotopic signatures was adjusted during the calibration process along with the form (magnitude and timing) of each nitrate source flux.

Table 3

Table 4

2.4.2 Groundwater recharge

Recharge is the process by which groundwater is replenished by the infiltration of precipitation that reaches the aquifer. Groundwater recharge used as input for the deep model was obtained from Paradis et al. (2016) that computed daily values with the physically-based quasi two-dimensional infiltration model HELP (Schroeder et al., 1994) for all of PEI at a 0.25 km^2 spatial resolution. In this previous study, recharge estimates from HELP were calibrated against baseflow for the major rivers assuming that baseflow is an approximation for the average groundwater recharge over the entire watershed (Risser et al., 2005). Using weather data, HELP can simulate daily movement of water in the soil and accounts for surface storage, snowmelt, runoff, infiltration, evapotranspiration, vegetative growth, soil-moisture and lateral subsurface drainage. Specifically, annual groundwater recharge values simulated with HELP for the Wilmot watershed are comparable to baseflow values estimated from the analysis of the streamflow components (direct precipitation, runoff, baseflow) of the Wilmot River (r=0.69 for the 1972-1999 period). Details about HELP and its application for PEI can be found in Paradis et al. (2016).

To simulate scenarios of nitrate flux leaching to groundwater with the deep model (see Section *Calibration of local-scale seasonal fluxes from nitrate sources*), the average recharge value of 410 mm y^{-1} obtained by Paradis et al. (2016) for the 1972-1999 period was used, given the fact that no long-term trends were observed in annual recharge values and mean annual water table levels for the available observation period. For the detailed simulation of the nitrate sources with the shallow model (see Section *Simulation of flux from nitrate sources*), daily recharge was used for the 2-year period corresponding to the groundwater sampling period (from June 1, 2003, through May 31, 2005). Over a year, spring is usually the main recharge period, but here the end of fall also brings a significant amount of water. For these two years of sampling, annual recharge was respectively 316 mm y^{-1} and 237 mm y^{-1}, which is below the historic average value of 410 mm y^{-1}. For the two models, the recharge was applied uniformly over the watershed, given the relative homogeneity of the land use, vegetation, terrain slope, soil type and precipitation. Note that groundwater recharge estimated with HELP was not modified during calibration because of its fairly good correlation with independent estimates of groundwater recharge (baseflow).

2.4.3 Nitrogen available for leaching to groundwater

To reproduce the recent trend in increasing nitrate concentration observed in water (Somers et al., 1999) with the deep numerical model, the historical nitrate flux leaching to groundwater needs to be estimated. Since no record of this flux is available for the Wilmot watershed, the mass of N available for leaching to groundwater is used as an index of potential groundwater contamination by nitrate. The N available to leaching is water soluble inorganic N (ammonium and nitrate) spread over agriculture lands, and can leach through the soil to reach groundwater (De Jong et al., 2008). To reconstruct a representative historical record of nitrate loadings for the watershed, the study used all available information and even some values or trends available in a nearby watershed, as described as follows (Table 5 and Figure 5):

- The 2000-2005 period: The estimate of the 2000-2005 period mass of N available for leaching was based on the agronomic mass balance made by Somers et al. (2007) for the Wilmot watershed. The calculation uses the quantities, timing and cropping practices associated with various N sources for the main crops throughout the entire watershed. The mass balance takes into account three major N sources: chemical fertilizers, manure and vegetal crop residues (including N fixed by legume plants and direct atmospheric deposition). The agronomic model also provides an estimate of the N available for leaching based on the portion of nitrate input that is harvested. The 2000-2005 period mass of N available for leaching was then estimated at 313,000 kg yr^{-1} for the watershed.

- The 1980-2000 period: The second estimation of N available for leaching is based on the Census of Agriculture for crop areas (AAFC, 2004). It was shown that the cultivated potato area for PEI was approximately 25,000 hectares in 1981 which increased to almost 45,000 hectares in 1996. Estimating an increase proportional to the PEI potato crop area for the Wilmot watershed, it was assumed that the mass of N available for leaching would have gone from approximately 190,000 kg yr^{-1} in 1981 to 313,000 kg yr^{-1} in 2000.
- The pre-1965 period: The world-wide introduction of chemical fertilizers as a means to increase agricultural production occurred in 1955 (Galloway and Cowling, 2002). In PEI, it is known from local producers that such fertilizer application practices were introduced around 1965. This information allows estimation of the third historical period related to the pre-1965 agricultural practices. For that period, the authors estimated the mass of nitrate leaching (instead of N available) to groundwater from a steady-state groundwater flow and nitrate transport simulation that represents the background nitrate concentration in the Wilmot River. This concentration was assumed to be less than 2 mg L^{-1}, which is based on the nitrate concentration measured in the Dunk River for the same period. The Dunk River is adjacent to the Wilmot River and shows similar hydrogeological and land use characteristics. The mass of nitrate leaching to groundwater modelled for that period was thus 41,400 kg yr^{-1}.

- The 1965-1980 period: Finally, since no relevant piece of information is available for that period, the mass of N available for leaching was linearly interpolated between 1965 and 1980 to reflect the gradual intensification of agriculture and chemical fertilizer use during the 1970s.

This reconstructed historical record was used as a first approximation of the mass of nitrate leaching to groundwater with the deep numerical model, and it was further adjusted during calibration with nitrate concentration measured in surface water (see Section *Calibration of hydraulic properties*).

Table 5

2.5 Model calibration

Large uncertainties are generally associated with hydraulic parameters and inputs of numerical flow and transport models because of the incomplete knowledge on the flow system, which is complex in terms of geology and physical processes. Model calibration and sensitivity analysis are thus required to identify the most representative model parameters and inputs, based on the comparison of model outputs with field observations of hydraulic heads, solute concentrations and mass fluxes (water and solute) in the aquifer (Anderson et al., 2015). The problem of equi-finality associated with the calibration of a model having a large number of parameters was mitigated by constraining parameter values within physically plausible ranges, based on the context of the study area or reported field values. Also, a multi-objectives calibration approach was adopted, using five independent data sets to constrain as much as possible the range of model parameter values.

2.5.1 Calibration of model parameters

Calibration of the two numerical models involved the use of hydraulic heads measured in domestic wells, groundwater ages derived from isotopic analysis, and baseflow recessions for the Wilmot River observed during low-flow periods. Calibration of the deep model involved the following steps:

- *Static hydraulic heads*: Using steady-state groundwater flow conditions, the hydraulic conductivities used in the numerical model were adjusted by comparing the simulated water table elevation to hydraulic heads measured in 243 domestic wells. Those wells are open boreholes in the sandstone aquifer. The average length of the open sections is 19 m (with a standard deviation of 14 m) and thus measured heads approximately represent the average head for the first two layers of the numerical model. Also, given the non-uniqueness in the paired hydraulic conductivity and recharge values, groundwater recharge was fixed to the average value of 410 mm y^{-1} corresponding to the 1972-1999 period that was estimated by HELP (see Section *Groundwater recharge*).
- *Groundwater age*: The calibration of the groundwater age profile measured at WIL-2 (see Section *Calibration of hydraulic properties*) was especially useful to adjust vertical hydraulic conductivities and thus better constrain nitrate migration at depth. This was carried out using the technique of Goode (1996) that uses an advection-dispersion transport equation to simulate groundwater age with a distributed zero-order source of unit strength corresponding to the rate of aging. In this approach, the dependent variable is the mean age (instead of the solute concentration), which is a mass-weighted average age. The "age mass" is the product of the mass of water and its age, and the age mass is assumed to be

conserved during mixing. Boundary conditions include zero age mass flux across all no-flow and inflow boundaries and no age mass dispersive flux across outflow boundaries. The solution of the governing transport equation yields the spatial distribution of the mean groundwater age under steady-state flow conditions, considering the processes of diffusion, dispersion, mixing and exchange. From the previously calibrated steady-state groundwater flow model with heads, a steady-state mass transport problem was defined with the groundwater recharge boundary as a zero-mass age flux and the constant heads as no age mass dispersive flux. The material conditions corresponding to the source term of zero order was set at 17% (equal to *n*). The effective diffusion coefficient was $1x10^{-9}$ m^2 s^{-1} and longitudinal and transverse dispersion were set respectively at 5 and 0.5 m considering the scale of the system (Gelhar et al., 1992), assuming that dispersions of solutes and dating indicators are the same.

Calibration of the shallow model involved the following steps:

- *Static hydraulic heads*: While the trend in *K* with depth for the sub-model was slightly modified with respect to the deep model, the overall transmissivity of the HF interval was kept similar in order not to alter the deep model calibration values.
- *Baseflow recessions*: A baseflow recession is the decline in streamflow that a river would produce when only groundwater is contributing to the streamflow and the aquifer is under continuous conditions of no recharge (Gburek et al., 1999). For the Wilmot watershed, this condition is often observed during the summer months when evapotranspiration is high and there is no precipitation for several days. Calibration of the numerical model with

baseflow recessions provides an estimate of the global S_y of the aquifer, which is an important parameter that controls groundwater residence time. Six baseflow recessions lasting between 14 and 97 days were extracted from the streamflow record of the Wilmot River for the period of 1972 to 1996. To model the recessions, hydraulic heads of the groundwater flow model after calibration with heads and groundwater age were used as initial conditions for a 100-day transient simulation without recharge. S_y was then manually adjusted until simulated baseflow recessions reproduced observations. For this calibration, it is assumed that the hydraulic connection between the aquifer and the river is direct and that bank storage effects are negligible, which is a reasonable assumption for the Wilmot River given that its floodplain is poorly developed with respect to the main river channel.

2.5.2 Reconstruction of the historical nitrate flux leaching to groundwater

Given the large uncertainties in the historical nitrate flux leaching to groundwater, the historical flux of the deep model was adjusted with surface water nitrate concentration records. While only limited data exist for groundwater nitrate concentration in the Wilmot watershed (mostly groundwater records for the 2002-2004 period), nitrate concentration records for the Wilmot River and the nearby Dunk River exist for longer periods (1992 to 2000 and 1973 to 2000, respectively). The close relationship between groundwater and surface water nitrate concentration supported the use of surface water records for the calibration of the historical nitrate flux to groundwater. Moreover, statistical analysis for the overlapping records of the Dunk and Wilmot Rivers showed that they have similar temporal trends, with average nitrate concentration for the Wilmot River being about 1.5 mg L^{-1} higher than for the Dunk River (Figure 5). This allowed the use of the Dunk River nitrate concentration record as a proxy for the Wilmot River after proper scaling. Then, the initial estimate of the historical nitrate flux was manually adjusted to reproduce the trend in nitrate concentration measured in the Wilmot River, while keeping the previously calibrated model parameters unchanged. A *n* of 17%, an effective diffusion coefficient of 9.8×10^{-11} m^2 s^{-1}, and a longitudinal and transversal dispersion of 5 and 0.5 m were used. Considering that agricultural activities use 76% of the watershed surface, the historical nitrate flux was applied uniformly over the surface of the numerical model.

2.5.3 Simulation of flux from nitrate sources

To model the dynamics of nitrate production and leaching to the aquifer, the shallow model was used to reproduce the total nitrate concentration and the proportion of the three main nitrate sources (chemical fertilizers, manure and soil organic matter) to the load in groundwater, which were determined with nitrate isotopic data over the two-year period of sampling (see Section *Nitrate sources in groundwater from isotopes*). To represent the short-term changes in total nitrate concentration and nitrate source proportions, transient simulations for both groundwater flow and nitrate transport were carried out, using daily groundwater recharge independently derived from the HELP model (see Section *Groundwater recharge*).

Transient transport simulations were carried out for loading from each individual nitrate source to reproduce its measured equivalent seasonal concentration. Daily nitrate fluxes were defined to match the time step of daily recharge provided by the HELP infiltration model. In the numerical model, the mass of nitrate was applied as a Neumann condition (mass flux) at the surface of the model, independent of groundwater recharge, which allows one to take into account the dilution effect of recharge on nitrate concentration. To simplify the calibration process, the form of each nitrate source was defined as step functions (Figure 6), although gradual changes in nitrate production and leaching are expected in the natural system. The initial nitrate mass flux functions were based on isotopic results of Savard et al. (2007) following a three-step process. First, the nitrate proportion from each nitrate source was used to apportion their respective seasonal loading based on total concentration, thus providing an equivalent concentration. Second, an estimate of the seasonal mass yield for each source was obtained from the product of concentration by the seasonal recharge rate. Third, the nitrate mass flux was obtained from the ratio of total load by the number of days of source application and recharge considered. An automatic time-step control scheme was used for time discretization of both transient simulations.

2.5.4 Calibration assessment

Model calibration performances with the different data sets were assessed with mean difference (M), coefficient of determination (C_D) and correlation coefficient (r), as defined by Smith et al. (1997). M, the mean difference between measured and simulated values, gives an indication of the bias in the simulation. A null M value indicates that there is no systematic bias. C_D measures the proportion of the total variance in the observed data that is explained by the predicted data. Note that C_D uses the explained sum of squares (instead of the more conventional residual sum of squares) as this representation allows a better comparison between the total variances of the observations and model predictions (Smith et al., 1997). Thus, C_D can range from 0 to any positive number, and a value greater than 1 indicates that the model describes the measured data better than the mean of the measurements. The r is used to assess whether simulated values follow the same pattern as measured values. The closer r is to 1, the better the model reproduces the trend in the observations. Thus, the calibration process aims at zeroing M and maximizing C_D and r. For semi-quantitative groundwater age data, a visual analysis between simulated and measured profiles was used because the ^{14}C data do not provide precise estimates of groundwater residence time (Clark and Fritz, 1997).

2.6 Scenarios of nitrate flux leaching to groundwater

Three different scenarios of future nitrate flux leaching to groundwater were simulated with the deep model to evaluate the potential impact of changes in agricultural practices over the 2000 to 2055 period (55 years) on nitrate concentration in groundwater:

- Maintain the 2000 agricultural practices (Scenario 2000): The estimated mass of nitrate reaching the aquifer in 2000 is kept constant until 2055.
- Maintain current agricultural growing trend (Scenario TREND): A 23% increase in mass for 2050 relative to the 2000 nitrate load. This percentage corresponds roughly to the increase observed in the 10-15 years prior to 2000.
- Total stop of nitrate flux leaching to the aquifer (Scenario CLEAN): The mass of nitrate applied is abruptly stopped in 2000, which may involve cessation of all agricultural activities or perfectly efficient BMP. This scenario is not realistic but it was simulated to further assess the lag time between reductions in the nitrate load at the water table and lowering of nitrate concentration in the upper part of the aquifer exploited by domestic wells for drinking water.

Nitrate flux for each scenario was applied uniformly over the entire watershed given the widespread nature of agricultural activities over the Wilmot watershed. The three scenarios were simulated under steady-state flow and transient nitrate mass transport conditions with the year 2000 hydraulic heads and nitrate concentrations used as initial conditions. An automatic time-step control scheme was also used for time discretization of the transport simulations.

3 Results and discussion

3.1 Calibration of hydraulic properties

Under steady-state flow conditions, simulated heads and measured heads in domestic wells with the deep model are in close agreement (Table 6). Calibrated parameters (Table 3) led to high values of *r* and *CD*, at 0.93 and 6.3, respectively, but to a moderate bias. Nearly identical calibration performances (not shown) were obtained with model parameters shown in Table 4 for the shallow model simulating nitrate loads from sources (see Section *Simulation of flux from nitrate sources*). Those calibration performances are acceptable, considering that head data are from measurements in domestic wells that were taken at different periods of the year (annual water table fluctuations are generally around 1 m), associated with a drilling period that spanned several decades (from 1959 to 2003).

For the calibration with groundwater ages, Figure 4 compares the groundwater age simulation with indications of age obtained from tritium and ^{14}C analyses at well WIL-2. It was observed that the simulated age with the deep model is in agreement with tritium values suggesting that groundwater is younger than 50 years in the HF interval. Also, the simulated age in the LF interval with values up to 1,500 years is in the same order of magnitude as corrected ^{14}C age, ranging from 2,000 to 3,000 years. Thus, while the simulated age appears slightly underestimated with respect to corrected ^{14}C values, the model is reproducing the general trend in groundwater age with modern groundwater in the HF interval and much older groundwater in the LF interval. Sensitivity simulations have shown that K_h, K_v and S_y values of the first two model layers of the shallow model are mostly controlling baseflow recession curves, indicating a hydraulic link between the surficial

HF interval and the Wilmot River. Note that the movable mesh feature in FEFLOW allows the specification of unconfined conditions for multiple layers when the water table fluctuations span over many layers. This explains the sensitivity of baseflow recessions with the properties of the top two layers. Note also that storage properties for deeper layers were not calibrated because the volume of water released from these deep layers was too small compared to the top layers, thus storage properties of deeper layers did not impact baseflow recessions that were used to calibrate these properties. Interestingly, the best calibration results (Table 6) were obtained for S_y values close to 1% (Table 4), even though *n* is as high as 17%. This specific yield, actively contributing to groundwater flow, is attributed to sandstone fractures. Simulated baseflow recessions were in very close agreement with observed recessions in the Wilmot River (high values of *r* and *CD*, Table 6), without systematic bias. This strong agreement is the result of the recharge calibration obtained from the HELP model (see Section *Groundwater recharge*) that made use of baseflow data from all major rivers on PEI (including the Wilmot River). This result shows that the change in model scale from the entire PEI to the watershed scale did not alter recharge estimates significantly.

3.2 Calibration of watershed-scale historical nitrate mass leaching

Transient mass-transport simulations were carried out to achieve nitrate concentration calibration with the deep model (Table 6); these show that 93% of the 2000-2005 period's initial N mass available for leaching in the Wilmot watershed (Somers et al., 2007) is needed to reproduce nitrate concentrations observed in the Wilmot River (Figure 5). This appraisal agrees with an independent estimate suggesting that 87 to 96% of soil-N annually available to leaching as nitrate is reaching groundwater in PEI (De Jong et al., 2008), which suggests a very low denitrification rate in the soil layer. The simulated yearly trend from 1973 to present is in good agreement with nitrate concentrations measured in the Wilmot River (Figure 5). Even though there is only a slight bias in simulated and observed nitrate concentrations, r and C_D are the weakest compared with other calibration parameters. This could be attributed to the nitrate concentration measured in rivers that may show higher variability due to a varying degree of dilution with runoff water at different sampling periods. So, diluted samples would lead to lower nitrate concentration.

3.3 Calibration of local-scale seasonal fluxes from nitrate sources

Figure 6 shows that total and individual concentrations simulated for each nitrate source with the shallow model nicely compare with observations in domestic wells. Simulated concentrations are averaged for the 5 layers of the model, weighted by layer transmissivities at the 16 observation points where sampled domestic wells are located. These calibrated results were obtained by iteratively adjusting the magnitude and timing of nitrate mass fluxes as well as model parameter values for n and S_y; the best fit was obtained for n and S_y of 2% and 1.5%, respectively (Table 4). The S_y value used was previously obtained through calibration with baseflow recessions and a modification of this value did not provide a better match. The K_h profile was also modified to better match the nitrate mass flux timing. In comparison with the deep model, the overall transmissivity for the same interval was similar and only the general vertical trend was modified.

Thus, in spite of simplification of physical processes and uncertainty in hydraulic parameter values and spatial variability, calibration results suggest that the numerical models can be used to adequately represent the main nitrate transport mechanisms in the Wilmot aquifer.

Table 6

Figure 4

Figure 5

Figure 6

3.4 Groundwater nitrate transfer to river and distribution within the aquifer

Figure 7 presents particle tracking carried out through the WIL-1 to WIL-3 transect for three different depths within the deep model providing an appreciation of the link between the aquifer and the Wilmot River. Based on the small travel path envelope and the short travel time (less than 20 years), it appears that the HF interval (model layer 1; Figure 7a) is well connected to the Wilmot River and that groundwater mostly flows directly to the river within this interval. The LF shallow interval (model layer 5; Figure 7b) is also connected to the Wilmot River but it provides much less contribution and takes a travel time of up to 10 000 years to reach the river, while particle tracking for the LF deep interval (model layer 7; Figure 7c) suggests that the aquifer is draining much farther down-gradient and closer to the estuary. Moreover, the simulated nitrate concentrations for year 2000 within the Wilmot aquifer at a transect crossing WIL-1 to WIL-3 show that the concentrations are homogeneously distributed (Figure 8), owing to the homogeneous flux and parameters used in the model. The highest concentrations are found in the HF interval (model layers 1-4) with a drastic decrease below that interval. Thus, this suggests that nitrate is transported to the Wilmot River mostly through the HF interval where nitrate contamination is mostly restricted. Also, the limited mass of nitrate transferred to deeper intervals is due to the strong *K* anisotropy that limits vertical advective nitrate migration.

Figure 7

Figure 8

3.5 Watershed-scale simulations of nitrate leaching and transport

Figures 9a, 9b and 9c show the mean nitrate concentrations simulated for the first five upper layers of the deep numerical model according to the three nitrate leaching scenarios. The simulated nitrate concentration for layers 1 to 4 are representative of the nitrate concentration found in most domestic wells of the region because the total thickness of those layers spans similar depths. The nitrate load applied to the model for each scenario is calculated from the load obtained after calibration (see Section *Calibration of hydraulic properties*). As shown, the scenarios have different impacts on the nitrate concentration in groundwater at the scale of the watershed:

- Scenario 2000 maintained the 2000 agricultural practices beyond year 2000 with an estimated nitrate load of 292 000 kg yr^{-1} and leads to an increase in average nitrate concentration for layers 1 to 4 from 4.8 to 6.6 mg L^{-1} in 2000 to almost constant values between 7.9 and 8.3 mg L^{-1} in 2055. Even though the applied nitrate load is constant over the years, average nitrate concentration keeps increasing in drinking water for about 25 years beyond year 2000 until an equilibrium in nitrate concentration is reached between fracture flow and mass accumulated in the porous sandstone matrix. For layer 5, the time to reach concentration equilibrium is longer, and average nitrate concentration increases from 0.3 mg L^{-1} in 2000 to 2.6 mg L-1 in 2055, without yet reaching a constant concentration. This difference in time required to reach equilibrium is explained by the fact that groundwater flow in the shallow LF interval (model layer 5) is much slower than for the upper HF interval due to relative differences in *K* and depth. Those results show that maintaining the 2000 nitrate loading would seem to provide an apparently safe level of nitrate concentration in groundwater used for drinking purposes because average nitrate concentration would not exceed the health recommendation of 10 mg L^{-1}. However, the numerical model does not represent the spatial variability in nitrate concentration in the watershed. Knowing that, today, over 20% of the wells show nitrate concentration exceeding the health recommendation (Savard et al., 2004), an increase in the average nitrate concentration would lead to a higher proportion of wells exceeding that limit.

- Scenario TREND maintained the current agricultural growing trend in nitrate loading beyond year 2000 and shows that a 23% increase (from 292 000 kg yr^{-1} in 2000 to 360 000 kg yr^{-1} in 2055) in the nitrate load would lead to an average nitrate concentration close to 10 mg L^{-1} in drinking water in 2055. This increase is the combined effect of increasing nitrate load combined with equilibration of the nitrate concentration. Under such conditions, most wells in the watershed would have nitrate concentration near or exceeding the recommended maximum for nitrate concentration. Groundwater would thus generally be unsafe for drinking without treatment throughout most of the watershed. Moreover, average nitrate concentration for layer 5 is significantly lower than for the upper layers, which makes this part of the aquifer less vulnerable to surface contamination. That is, the migration of the nitrate at depth is relatively slow due to lower *K*, longer groundwater flow paths and important nitrate diffusion into the sandstone matrix.
- Scenario CLEAN involves stopping nitrate flux leaching to the aquifer beyond year 2000 and indicates that a time of about 20 years (around year 2020) would be necessary to reduce nitrate concentration to a background level lower than 1 mg L^{-1} in groundwater used for

drinking (model layers 1 to 4). The pattern for layer 5 is however very different, with a steady increase in nitrate concentration and a delay of 30 years until a maximum value up to 1 mg L^{-1} is reached, followed by a very slow decrease thereafter. This illustrates that while the more active groundwater flow interval (model layers 1 to 4) could be cleaned from contamination more rapidly, the contamination at depth in the less active interval (model layer 5) is more persistent. Simulations assumed that diffusion occurs instantaneously, and for cases where the diffusion would not be complete due to groundwater residence times shorter than diffusion times, the clean-up time could only be shorter.

The simulated scenarios for estimating future nitrate concentration in groundwater demonstrate that even a sharp decrease in nitrate loadings would still lead to continued concentration increase over the next 25 years due to the specific dynamics of the Wilmot aquifer. This means that changes in groundwater quality following a modification of the agricultural practices could only be observed after several years of implementation. Furthermore, to maintain the average nitrate concentration at its current level, it would be necessary to reduce the nitrate load below its 2000-2005 period value.

Those results have to be compared with the work of Jiang et al. (2009), which provided similar scenarios for the Wilmot aquifer. With their finite-difference hydrogeological model, Jiang et al. (2009) found lower future nitrate concentrations and faster responses to changes in nitrate loadings. This difference with the present study mainly stems from the higher S_y (6% instead of 1% in this study) and lower *n* (7% instead of 17%) used by Jiang et al. (2009), which results in an aquifer draining more rapidly and storing less nitrate by diffusion in the matrix. Those discrepancies could be attributed to a model calibration approach using less calibration targets than the one applied over the course of the present study. Nevertheless, a wise use of hydrogeological models to design agricultural and water management plans would use all available models to assess uncertainty in model predictions before taking any actions.

Finally, since the end of this project in 2006, nitrate concentrations in the Wilmot River steadily increased from 2006 to 2017 and have since then slightly decreased. For instance, annual average concentrations have risen to over 7 mg L^{-1} in the river to finally stabilize at around 6 mg L^{-1} in 2016, which is approximatively 0.5 mg L^{-1} over the 2000 level (Q. Li and C. Crane, Prince Edward Island Department of Communities, Land and Environment, personal communication, 2017). A similar trend was also observed with nitrate concentrations in wells. Those observed trends, compared to simulated concentrations, suggest that the agricultural practices over the Wilmot watershed may have involved a slight reduction in N loads or loads similar to the ones applied in 2000, as shown for Scenario 2000 (Figure 9a). The cause of this change is not well understood, but it potentially results from a better awareness by farmers of the impact of fertilizer application on water quality, the economic demand for agriculture goods, the limited possible further expansion of farmland, and/or variations in climatic and recharge conditions.

Figure 9

3.6 Seasonality of nitrate sources and transformation

The similar *n* and S_y calibrated values (2% versus 1.5%, respectively) obtained by modeling the sources of nitrate using isotopic data with the shallow model (see Section *Simulation of flux from nitrate sources*) suggests that short-term nitrate transport is essentially controlled by the fractures with little influence from the porous matrix. The residence time of the water in fractures pumped out at the domestic wells is likely not long enough for diffusion to occur, as also suggested by the strong seasonality of the isotopic nitrate data which closely matches the fertilizer application practices. Longer residence times would have led to damped isotopic signals. The seasonality in nitrate source inputs could also be explained by the fact that the relatively large annual recharge (277 mm y^{-1} for the 2-year sampling period and 410 mm y^{-1} on average) corresponds to up to twice the S_y of fractures in the HF interval. This condition leads to a rapid substitution of the groundwater present in fractures of the HF interval by recharge, which induces rapid seasonal changes in groundwater nitrate concentration and source proportions according to the variations in nitrate fluxes from chemical fertilizers, manure and soil organic matter. The seasonality is also magnified by the fact that younger waters are entering the aquifer by its more permeable zone at the top of the HF interval. So, when groundwater is pumped, more water is coming from this zone due to its higher transmissivity and thus dominates the isotopic signal.

Figure 10 compares the agronomic N mass balance for the Wilmot River watershed estimated by Somers et al. (2007) to the proportions of nitrate sources in groundwater estimated with the shallow model. For the development of the N mass balance, Somers et al. (2007) collected data for estimating the proportions of the watershed occupied by specific land uses within the watershed, representative input and output rates for the main N sources and sinks, and the timing and prevalence of the main agronomic practices. The mass balance considered chemical fertilizers, organic sources (manure and domestic sewage), crop residues and direct atmospheric deposition. The mass balance results represent the proportion of the sources of nitrate applied as fertilizers that could have leached to the aquifer, while modeling results represent the proportions of the nitrate mass originating from these sources that have actually reached the aquifer. Comparison of these proportions thus allows inference of the proportions of chemical and manure fertilizers that were integrated into vegetal and organic matter prior to their nitrification and leaching to the aquifer. More than 50% of the nitrate originates from chemical fertilizers, which only represents about 25% of the nitrate found in the groundwater, thus implying a 50% transformation into vegetal and soil organic matter prior to leaching to groundwater (Figure 10). A similar process is inferred to occur for manure. The year-long transformation of soil organic matter (including crop residues) into leachable nitrate, even during winter months, and the large proportion of nitrate originating from this source suggest removal of crop residues or restricting ploughing during spring as two easily applicable practical means for reducing nitrate leaching.

Figure 10

4 Summary

The development of groundwater flow and nitrate transport numerical models tracking back historical nitrate loadings to reproduce the 2000 level of nitrate contamination in groundwater and surface water has led to a better understanding of nitrate transport mechanisms in the Wilmot watershed sandstone aquifer. Supported by a combination of field and laboratory measurements, and a comprehensive model calibration approach with multiple complementary datasets, the main nitrate transport characteristics of the Wilmot aquifer were deduced (Figure 11):

- Nitrate sources applied as chemical fertilizers and manure at the soil surface are transformed in part into soil organic matter (SOM) in the soil before being leached by recharge through weathered sandstone fractures. Most of the leached nitrate reaching the aquifer is then coming from a SOM source. See Fig 11a.
- Seasonal recharge brings nitrate into the shallow part of the aquifer (HF interval). Nitrate-carrying recharge quickly replaces the groundwater present in the permeable but low-porosity fracture system, so that diffusive exchange of nitrate between the porous matrix and fractures does not have time to alter the isotopic signal of nitrate leached from the soil. Nitrate found in domestic wells exploiting the HF interval has the isotopic signal of the nitrate sources leached from the soil by recharge. This makes domestic wells very vulnerable to surface agricultural contamination. See Fig 11b.
- At the scale of the watershed aquifer system, slowly migrating nitrate in the fracture system diffuses into the porous matrix, which retards nitrate migration and leads to a large accumulation of nitrate mass in the porous matrix of the aquifer. The nitrate mass discharging with groundwater into the Wilmot River thus has a large time lag with variations in the nitrate flux from the soil to the aquifer. Nitrate reaching the Wilmot River represents a mixture of nitrate having migrated with groundwaters of various residence times, which have flown through different parts of the aquifer system. However, surface water composition is dominated by groundwater coming from the HF interval due to its higher permeability and direct connection with the River. See Fig 11c.

Finally, modeling of the Wilmot aquifer allows a better understanding of the importance of advective and dispersive nitrate transport mechanisms. The findings of this study provide useful guidance to stakeholders responsible for agricultural and water management plans by highlighting the anticipated responses of the aquifer to different practical situations, but especially the lag time to be expected between BMP application and potential improvements in groundwater quality.

Figure 11

Acknowledgements

The authors would like to thank R.E. Jackson, V. Cloutier, G.H. Somers and Y. Jiang for their constructive discussions. The constructive comments from T. Cui and an anonymous reviewer were also appreciated. This study was funded in part by the Geological Survey of Canada from its Groundwater Mapping Program (Groundwater Earth Observation and Thematic Research), by the Prince Edward Island Ministry of Environment, Energy and Forestry, and by a NSERC Discovery Grant to R.L. This is ESS contribution number 20100143.

References

Agriculture and Agri-Food Canada (AAFC), 2004. Census of Agriculture: Soil Landscapes of Canada (SLC)-v.3 and Water Survey of Canada sub-sub drainage area (WSCSSDA)-v.5 http://sis.agr.gc.ca/cansis/nsdb/slc/index.html (last access: 8/8/17)

Anderson, M. P., Woessner, W. W., Randall, J. H., 2015. Applied Groundwater Modeling (Second Edition). Academic Press, San Diego.

Atlantic AgriTech (AAT), 2006. Agricultural land use practices in the Wilmot River watershed area of the Prince Edward Island. Report to the Prince Edward Island Department of Environment, Energy and Forestry, Charlottetown, Prince Edward Island , 22 p.

Beaudoin, N., Saad, J.K., Van Laethem, C., Machet, J.M., Maucorps, J., Mary, B., 2005. Nitrate leaching in intensive agriculture in Northern France: effect of farming practices, soils and crop rotations. Agric. Ecosyst. Environ. 111, 292-310.

Benson, V.S., VanLeeuwen, J.A., Sanchez, J., Dohoo, I.R., Somers, G.H., 2006. Spatial Analysis of Land Use Impact on Ground Water Nitrate Concentrations. J. Environ. Qual. 35, 421-432.

Blombäck, K., Eckersten, H., Lewan, E., Aronsson, H., 2003. Simulations of soil carbon and nitrogen dynamics during seven years in a catch crop experiment. Agric. Syst. 76, 95-114.

Bracmort, K.S., Arabi, M., Frankenberger, J.R., Engel, B.A., Arnold, J.G., 2006. Modeling long-term water quality impact of structural BMPs. Am. Soc. Agric. Biol. Eng. 49 (2), 367-374.

Clark, I.D., Fritz, P., 1997. Environmental Isotopes in Hydrogeology. CRC Press, Boca Raton, FL, USA, 328 pp.

Constantin, J., Mary, B., Laurent, F., Aubrion, G., Fontaine, A., Kerveillant, P., Beaudoin, N., 2010. Effects of catch crops, no till and reduced nitrogen fertilization on nitrogen leaching and balance in three long-term experiments. Agric. Ecosyst. Environ. 135, 268-278.

Cui, T., Yang, J., Samson, I., 2010. Numerical modeling of hydrothermal fluid flow in the Paleoproterozoic Thelon Basin, Nunavut, Canada. J. Geochem. Exploration, 106, 69-76.

Cui, T., Yang, J., Samson, I., 2012. Solute transport across basement/cover interfaces by buoyancy driven thermohaline convection: implications for the formation of unconformity-related uranium deposits. Am. J. Sci., 312, 994-1027.

De Jong, R., Qian, B., Yang, J. Y., 2008. Modelling nitrogen leaching in Prince Edward Island under Climate change scenarios. Can. J. Soil Sci. 88, 61-78.

Diersch, H.J.G., 2004. FEFLOW: Finite Element Subsurface Flow and Transport Simulation System – Reference Manual. WASY Institute for Water Resources Planning and System Research Ltd. 277 pp.

Dimitriou, E., Moussoulis, E., 2010. Hydrological and nitrogen distributed catchment modeling to assess the impact of future climate change at Trichonis Lake, western Greece. Hydrogeol. J. 18(2), 441-454.

Domenico, P.A., Schwartz, F.W., 1998. Physical and Chemical Hydrogeology. 2^{nd} edition, John Wiley and Sons, New York, 506 pp.

Francis, R.M., 1989. Hydrogeology of the Winter River Basin, Prince Edward Island. Department of the Environment, Water Resources Branch, Prince Edward Island, 117 pp.

Freeze, R.A., Cherry, J.A., 1979. Groundwater. Prentice-Hall, Inc. Englewood Cliffs, NJ, p. 604.

Furey, P.R., Gupta, V.K., 2001. A physically based filter for separating base flow from streamflow time series. Water Resour. Res. 11, 2709-2722.

Gburek, W.J., Folmar, G.J., Urban, J.B., 1999. Field data and ground water modeling in a layered fractured aquifer. Ground Water 2, 175-184.

Gelhar, L.W., Welty, C., Rehfeldt, K.R., 1992. A critical review of data on field-scale dispersion in aquifers. Water Resour. Res. 28(7), 1955-1974.

Goode, D.J., 1996. Direct simulation of groundwater age. Water Resour. Res. 2, 289-296.

Hattermann, F.F., V. Krysanova, A. Habeck, A. Bronstert. 2006. Integrating wetlands and riparian zones in river basin modelling, Ecological Modelling, 199(4), 379-392.

Health Canada, 2004. Summary of guidelines for Canadian drinking water quality; Prepared by the Federal–Provincial-Territorial Committee on Drinking Water of the Federal–Provincial-

Territorial Committee on Health and the Environment, April 2004, https://www.canada.ca/en/health-canada/services/environmental-workplace-health/reports-publications/water-quality/guidelines-canadian-drinking-water-quality-summary-table-health-canada-2012.html (last access: 8/8/17)

Keeney, D.R., Follett, R.F., 1991. Managing nitrogen for ground water quality and farm profitability: Overview and introduction. In: R.F. Follet et al. (eds) Managing nitrogen for ground water quality and farm profitability, 1–7. Soil Science Society of America, Madison, WI.

Kim, K., Anderson, M.P., Bowser, C. J., 1999. Model calibration with multiple targets: A case study. Ground Water 37(3), 1745-6584.

Laurent, F., Ruelland, D., 2011. Assessing impacts of alternative land use and agricultural practices on nitrate pollution at the catchment scale. J. Hydrol. 409, 440-450.

Liao, S.L., Savard, M.M., Somers, G.H., Paradis, D., Jiang, Y., 2005. Preliminary results from water-isotope characterization of groundwater, surface water, and precipitation in the Wilmot River watershed, Prince Edward Island. Geological Survey of Canada, Ottawa. Current Research 2005-D4, 10 p.

Lunn, R., Adams, R., Mackay, R., Dunn, S., 1996. Development and application of a nitrogen modelling system for large catchments. J. Hydrol. 174, 285-304.

Millington, R.J., Quirk, J.P., 1961. Permeability of porous solids. Transaction of Faraday Society 57, 1200-1206.

Molénat, J., Gascuel-Odoux, C., 2002. Modelling flow and nitrate transport in groundwater for the prediction of water travel times and of consequences of land use on water quality. Hydrological Process. 16, 479-492.

Mutch, R.D.Jr., Scott, J.I., 1993. Cleanup of fractured rock aquifers: implications of matrix diffusion. Environ. Monit. Assess. 24, 45-70.

Pankow, J.F., and Cherry, J.A., 1996. Dense Chlorinated Solvents and Other DNAPLs in Groundwater: History, Behavior, and Remediation. Waterloo Press, Ontario, 522p.

Paradis, D., Ballard, J.-M., Savard, M.M., Lefebvre, R., Jiang, Y., Somers, G., Liao, S.L., Rivard, C., 2006. Impact of agricultural activities on nitrates in ground and surface water in the Wilmot watershed, PEI, Canada. Sea to Sky Geotechnique 2006: proceedings of the 59th Canadian Geotechnical Conference and the 7th joint CGS/IAH-CNC Groundwater Specialty Conference. 2006 p. 1308-1315.

Paradis, D., Lefebvre, R., 2013. Single-well interference slug tests to assess the vertical hydraulic conductivity of unconsolidated aquifers. J. Hydrol. 478, 102-118.

Paradis, D., Vigneault, H., Lefebvre, R., Savard, M.M., Ballard, J.-M., Qian, B., 2016. Groundwater nitrate concentration evolution under climate change and agricultural adaptation scenarios: Prince Edward Island, Canada. Earth Syst. Dynam. 7, 183-202.

Prest, V.K., 1973. Surficial deposits of Prince Edward Island. Geological Survey of Canada, Ottawa, “A” Series Map 1366A.

Rode, M., Thiel, E., Franko, U., Wenk, G., Hesser, F., 2009. Impact of selected agricultural management options on the reduction of nitrogen loads in three representative meso scale catchments in Central Germany. Sci. Total Environ. 407, 3459-3472.

Savard, M.M., Somers, G.H., 2007. Consequences of climatic changes on contamination of drinking water by nitrate on Prince Edward Island. Earth Sciences Sector report, Ottawa, 142 p.

Savard, M.M., Paradis, D., Somers, G., Liao, S., van Bochove, E., 2007. Winter nitrification contributes to excess NO_3^- in groundwater of an agricultural region: A dual-isotope study. Water Resour. Res. 43, W06422.

Savard, M.M., Simpson, S., Smirnoff, A., Paradis, D., Somers, G.H., van Bochove, E., Thériault, G., 2004. A study of the Nitrogen cycle in the Wilmot River Watershed, Prince Edward Island: Initial Results. Fifth Joint CGS/IAH-CNC Conference GeoQuébec 2004, session 4A on water quality, pp. 20-27.

Savard, M.M., Somers, G., Smirnoff, A., Paradis, D., van Bochove, E., Liao, S.L., 2010. Nitrate isotopes unveil distinct seasonal N-sources and the critical role of crop residues in groundwater contamination. J. Hydrol. 381(1-2), 134-141.

Somers, G.H., 1992. Agricultural impacts on water quality - A Prince Edward Island perspective. Proceedings of the National workshop on Agricultural Impacts on Water Quality: Canadian Perspectives, CARP, Ottawa, Ontario, April, 1992, 8 pp.

Somers, G.H., 1998. Distribution and trends for the occurrence of nitrate in Prince Edward Island groundwater. *in* Proceeding from nitrate-agricultural sources and fate in the environment - Perspectives and Direction, Eastern Canada Soil and Water Conservation Center, Grand Falls, New Brunswick, February 26, pp. 19-26.

Somers, G.H., Raymond, B., Uhlman, W., 1999. Prince Edward Island water quality interpretative report 99. Prepared for Canada-Prince Edward Island Water Annex to the Federal/Provincial Framework Agreement for Environmental Cooperation in Atlantic Canada, 67 pp.

Somers, G., Savard, M.M., Paradis, D., 2007. Mass balance calculations to estimate nitrate proportions from various sources in the agricultural Wilmot watershed of Prince Edward Island. In: The 60th Canadian Geotechnical Conference & 8th joint GCS/IAH-CNC Groundwater Conference, Ottawa, Ontario, Canada, October 21–24, session T2-B on Source Water Protection, Abstract volume, pp. 112–118.

Vaché, K., Eilers, J., Santelmann, M., 2002. Water quality modeling of alternative agricultural scenarios in the US Corn Belt. JAWRA 38 (3), 773-787.

Vinten, A., Dunn, S., 2001. Assessing the effects of land use on temporal change in well water quality in a designated nitrate vulnerable zone. Sci. Total Environ 265, 253-268.

Van de Poll, H.W., 1983. Geology of Prince Edward Island; Prince Edward Island Department of Energy and Forestry, Energy and Minerals Branch, Charlottetown, 66 pp.

World Health Organization (WHO), 2007. Nitrate and nitrite in drinking-water: Background document for development of guidelines for drinking-water quality.

Wriedt, G., Rode, M., 2006. Modelling nitrate transport and turnover in a lowland catchment system. J. Hydrol. 328(1–2), 157-176.

Young, J., Somers, G.H., Raymond, B., 2003. Distribution and trends for nitrate in Prince Edward Island groundwater and surface waters; *in* Proceedings of 2002 National Conference on Agricultural Nutrients and their Impact on Rural Water Quality, pp. 313-319.

Table 1. Main characteristics of the Wilmot River watershed (flow rates are for the 1972-1999 period recorded at the 01CB004 station located above the tidally influenced portion of the river; Land uses are based on a LANDSAT image for year 2000).

Watershed physiography	**Wilmot River flow rate**	**Land use**
Area: 87 km^2 Average width: 5 km Average length: 17 km Elevation range: 0-90 masl	Mean annual: 0.92 $m^3\ s^{-1}$ Minimum monthly mean: 0.45 $m^3\ s^{-1}$ Maximum monthly mean: 1.88 $m^3\ s^{-1}$	Agriculture 76% Forest 11% Urban and roads 9% Wetland and recreational 4%

Table 2. Weather and water balance for the Wilmot River watershed (precipitation and evapotranspiration data are for the 1971-2000 period at the Summerside A station, and runoff and recharge data are estimated from the HELP model).

Watershed parameter	**Value**
Weather	
Mean annual total precipitation	1078 mm
Mean annual rainfall	809 mm
Mean annual snowfall	269 mm
Mean annual temperature	5.1 °C
Minimum mean monthly temperature	-8.6 °C
Maximum mean monthly temperature	18.4 °C
Water balance	
Mean annual evapotranspiration	438 mm

Mean annual runoff	230 mm
Mean annual recharge	410 mm

Table 3. Field-based and calibrated hydraulic parameter for the numerical model of the Wilmot aquifer used for the nitrate loading scenarios. K_h and K_v are respectively horizontal and vertical hydraulic conductivity (n.d.: not determined in the field for the deeper portions of the aquifer, but estimated from literature (Domenico and Schwartz, 1998)), n is total porosity and S_y specific yield.

Model Layer (Thickness in m)	**Flow Interval**	**Field K_h ($m\ s^{-1}$)**	**Watershed-scale numerical model**		
			K_h ($m\ s^{-1}$)	**K_v/K_h (-)**	**n (%)**
1 (3-12)	High Flow (HF)	$4.5x10^{-4}$ to $8.1x10^{-5}$	$3x10^{-4}$	1	17
2 (5)			$7x10^{-5}$	0.014	17
3 (5)			$7x10^{-6}$	0.01	17
4 (10)			$1x10^{-6}$	0.001	17
5 (25)	Shallow Low Flow (LF)	$1.7x10^{-4}$ to $8.4x10^{-7}$	$7x10^{-7}$	0.0014	17
6 (50)		n.d.	$1x10^{-7}$	0.5	17
7 (100)	Deep LF	n.d.	$5x10^{-8}$	1	17
8 (100)		n.d.	$1x10^{-8}$	1	17

Table 4. Field-based and calibrated hydraulic parameters for the numerical sub-model used to simulate isotopic data, for the High Flow (HF) interval. The bottom of this model falls approximately between layers 2 and 3 of the watershed-scale numerical model described in Table 3. The effective diffusion coefficient used is $1x10^{-9}\ m^2\ s^{-1}$, and longitudinal and transverse dispersivities are 5 and 0.5 m, respectively. Acronyms for hydraulic parameter are defined in Table 3.

HF: Model Layer (Thickness in m)	**Field K_h ($m\ s^{-1}$)**	**Numerical Sub-Model**			
		K_h ($m\ s^{-1}$)	**K_v/K_h (-)**	**S_y (%)**	**n (%)**
1 (>1)	$4.5x10^{-4}$ to $8.1x10^{-5}$	$6x10^{-4}$	1	1.5	2 (1 to 3)
2 (>1)		$5x10^{-4}$	0.1	1.5	2 (1 to 3)
3 (5)		$3x10^{-4}$	0.1	1.5	2 (1 to 3)
4 (5)		$1x10^{-4}$	0.01	1.5	2(1 to 3)
5 (5)		$5x10^{-5}$	0.01	1.5	2(1 to 3)

Table 5. Estimates of nitrogen available for leaching in groundwater and equivalent nitrate flux and concentration over the farming history of the Wilmot watershed. Note: calculations used a total watershed area of 87 km^2 and a mean annual recharge of 410 mm (Table 2).

Period	**Nitrogen available for leaching (kg yr^{-1})**	**Equivalent nitrate concentration (mg L^{-1} N-NO_3)**	**Wilmot potato farming area (hectare)**	**Basis for the estimate**
2000-2005	313,000	8.8	2000 (in 2000)	Mass balance (Somers *et al.*, 2007)
1980-2000	190,000 to 313,000	5.3 to 8.8	1114 (in 1981)	After PEI potato area census (AAFC, 2004)
1965-1980	41,400 to 190,000	1.2 to 5.3	-	Interpolation
Pre-1965	41,400	1.2	-	Numerical simulation (this study)

Table 6. Statistical analysis of model performance on calibration of different independent data sets for the simulation of groundwater flow and nitrate transport in the Wilmot aquifer system.

Calibration Target	**Model Performance**		
	Correlation Coefficient, *r*	**Mean Difference, *M***	**Coefficient of Determination, C_D**
Hydraulic heads	0.93	-3.42 m	6.3
Groundwater ages	Visual concordance		
Baseflow recessions	0.96	0.00 m^3 d^{-1}	10.6
Nitrate concentration in rivers	0.70	-0.31 mg L^{-1}	1.49
Nitrate proportions in groundwater	0.89	-0.02 mg L^{-1}	4.9

Figure 1. Map of the study area. The inset map shows the locations of Prince Edward Island and of the Wilmot River watershed. The study area map shows the physiography, land use and locations of different monitoring stations. Also indicated are the numerical model boundaries used to represent groundwater flow, nitrate mass transport and groundwater age.

Figure 2. Profiles of horizontal hydraulic conductivity (K_h) and hydraulic head (h) (relative to the mean sea level) measured between packers at observation wells (a) near the watershed divide (WIL-2) and (b) close to the Wilmot River (WIL-3) (locations shown in Figure 1). High flow (HF) and low flow (LF) intervals are indicated on the K_h profiles.

Figure 3. Monitoring of total nitrate concentration in groundwater and proportions of this concentration related to each nitrate source (chemical fertilizers, soil organic matter and manure) based on isotopic analyses of nitrate (Savard et al., 2007). The bars associated with total concentrations represent the standard deviation of measurements in the 16 domestic wells seasonally sampled from the summer of 2003 to the spring of 2005. Locations of sampled domestic wells are shown in Figure 1.

Figure 4. Simulated groundwater ages at a transect crossing observation wells (WIL-2, WIL1 and WIL-3) in the Wilmot River watershed compared to qualitative isotopic groundwater ages measured at WIL-3 (see Figure 1 for the transect location). Isotopic groundwater ages for the top four samples are based on tritium concentrations in tritium units (TU), whereas ^{14}C was used for the four deeper sampling points. ^{14}C is expressed in percent modern carbon (pMC). The second and third sampling points from the surface are inferred to represent mixtures (mix) of modern (<50 years) and old (>50 years) groundwaters.

Figure 5. Calibration of mean nitrate concentrations imposed on the model surface through time. The graph compares simulated (black line) and observed (grey squares) concentrations in the Wilmot River where the nitrate transported in groundwater discharges. Due to limited historical data for the Wilmot River, normalized nitrate concentrations for the adjacent Dunk River are also shown (black triangles). Dunk River concentrations were normalized based on their relationship with those of the Wilmot River for the period for which the data sets overlap. Also shown is the historical nitrogen available to leaching (dotted blue line) applied over the watershed as evaluated in Section *Nitrogen available for leaching to groundwater* and Table 5, and the calibrated nitrogen flux reaching the water table (solid blue line) through time obtained in the model. Both nitrogen available to leaching and nitrogen transformed in nitrate reaching the water table are expressed in concentration (left y-axis) and flux (right y-axis).

Figure 6. Calibrated (a) nitrate mass and groundwater recharge through time (2003 to 2005) used in the numerical model, to simulate the concentrations in shallow groundwater derived from the three main nitrate sources: (b) soil organic matter (SOM), (c) chemical fertilizers and (d) manure, whose sum gives the cumulative concentration in groundwater (e). (a) shows the input functions used for recharge, which were obtained from the HELP infiltration model, and the nitrate mass productions for each source represented by square functions. For three porosity values (n=1, 2 and 3%), the central three graphs compare simulated concentrations to values derived from nitrate isotopic analyses for each source (Figure 3). (e) illustrates simulated (n=2%) and observed total nitrate concentration and the proportions of the total concentration made up of each nitrate source. A specific storage (S_y) value of 1.5% was used for those simulations (Table 4).

Figure 7. Particles tracking for (a) the high flow (HF) interval (layer 1), (b) the low flow (LF) shallow interval (layer 5) and (c) the LF deep (layer 7) interval. Particles were released from a transect crossing WIL-1 to WIL-3. The figure shows the envelope of particle tracks and advective time isochrones for each flow system over the numerical grid shown in background.

Figure 8. Simulated nitrate concentration for year 2000 within the Wilmot aquifer along a transect crossing WIL-2 to WIL-3 (see Figure 1 for the transect location).

Figure 9. Simulated historical evolution of nitrate concentrations (Figure 5) up to year 2000, and prediction of the future evolution under three nitrate loadings scenarios showing average nitrate concentration in model layers 1 to 5: (a) Maintained current agricultural practices (2000) in the watershed and nitrate loading fixed at the one of year 2000; (b) Maintained current agricultural growing trend (TREND) with a 23% increase in mass for 2050 relative to the 2000 nitrate load and; (c) Assumes that nitrate loading is abruptly stopped in 2000 (CLEAN) and remains zero afterward. The dotted red line is the maximum recommended nitrate concentration in drinking water by Health Canada (2004).

Figure 10. Proportions of the sources of leached nitrate applied as fertilizers to soil (Somers et al., 2007) compared to the proportions from nitrate sources found in groundwater according to numerical modeling of nitrate source proportions derived from isotopic analyses (Savard et al., 2007). This comparison allows the inference of the transformation of chemical and manure fertilizers into soil organic matter prior to the leaching of nitrate to groundwater.

Figure 11. Conceptual model of nitrate transport in the Wilmot watershed aquifer system. (a) At the soil surface, applied nitrate sources (e.g., chemical fertilizers, manure and soil organic matter (SOM)) are either directly leached or transformed in the soil before being leached by infiltration through fractures. (b) Seasonal recharge brings nitrate into the shallow part of the aquifer and replaces groundwater present in the permeable but low-porosity fracture system. The thick replenished zone and the relatively slow process of diffusive exchange of nitrate between the porous matrix and fractures with respect to advective flow in fractures explain that nitrate found in domestic wells has the isotopic signal of the nitrate sources leached from the soil by recharge. (c) For groundwater having long residence time, which occurs at the scale of the watershed aquifer

system, diffusion of nitrate between the fracture system and the porous matrix occurs. This retards nitrate migration and leads to a large accumulation of nitrate mass in the porous matrix of the aquifer. Also, the larger permeability of the shallow aquifer creates a preferential nitrate migration path that discharge to the Wilmot River, and restrict nitrate transport at depth.

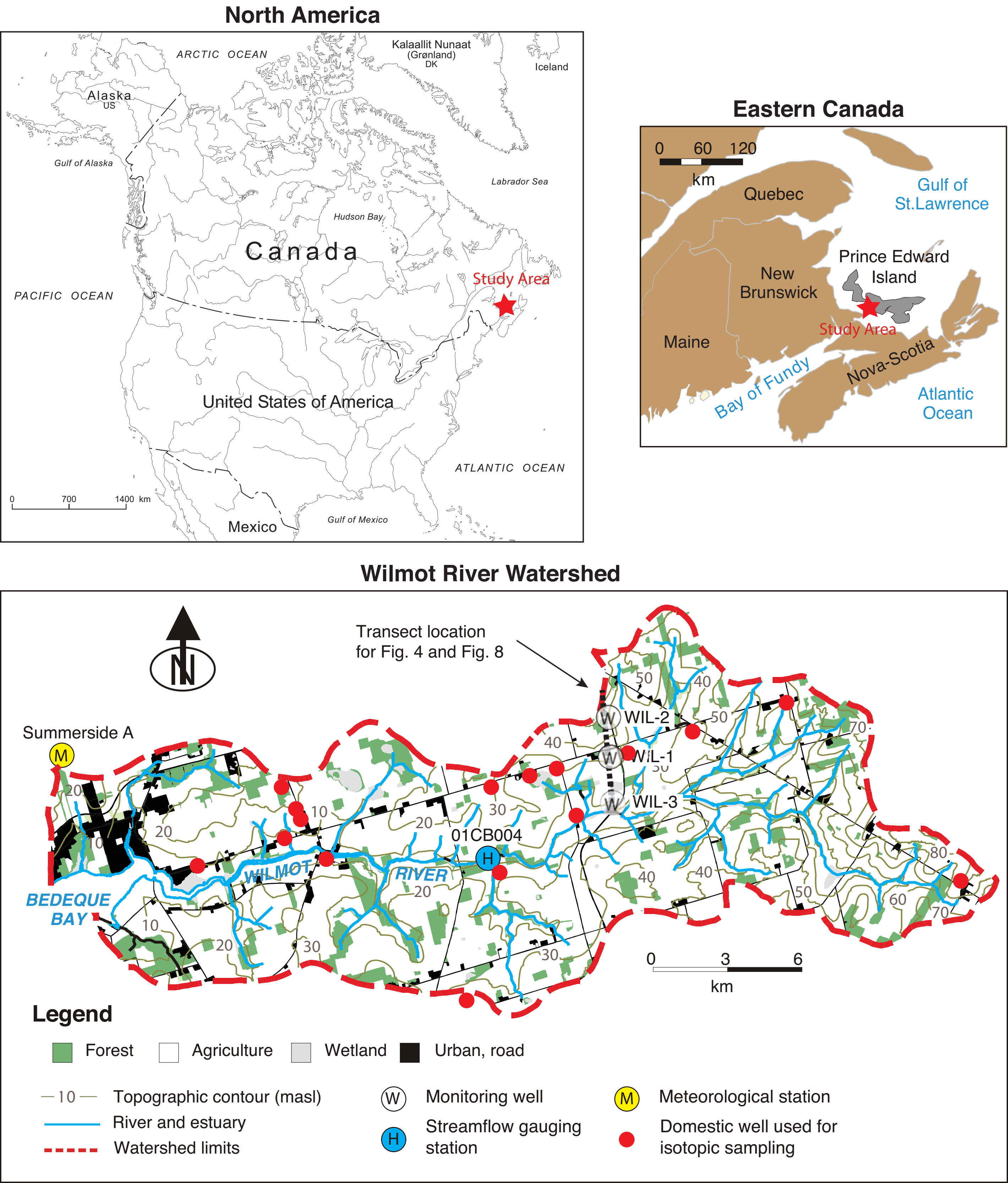
North America
ARCTIC OCEAN
Kalaallit Nunaat
(Grønland)
DK
Iceland
Alaska
US
Gulf of Alaska
Labrador Sea
Hudson Bay
Canada
Study Area
PACIFIC OCEAN
United States of America
ATLANTIC OCEAN
0
700
1400 km
Mexico
Gulf of Mexico
Eastern Canada
0
60
120
km
Quebec
Gulf of
St.Lawrence
Prince Edward
Island
New
Brunswick
Study Area
Maine
Nova-Scotia
Bay of Fundy
Atlantic
Ocean
Wilmot River Watershed
Transect location
for Fig. 4 and Fig. 8
N
Summerside A
M
WIL-2
WIL-1
WIL-3
01CB004
H
WILMOT
RIVER
BEDEQUE
BAY
10
20
30
40
50
60
70
80
0
3
6
km
Legend
Forest
Agriculture
Wetland
Urban, road
10
Topographic contour (masl)
River and estuary
Watershed limits
W
Monitoring well
H
Streamflow gauging
station
M
Meteorological station
Domestic well used for
isotopic sampling

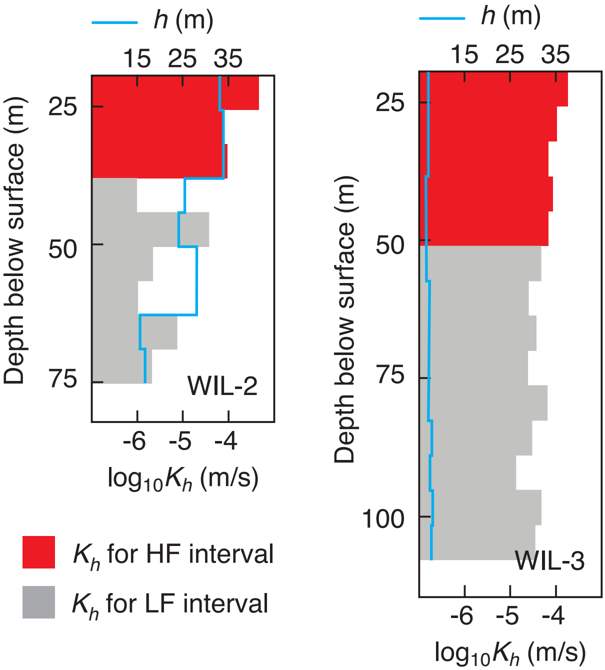
h (m)
15 25 35
Depth below surface (m)
25
50
75
WIL-2
-6 -5 -4
log10Kh (m/s)
h (m)
15 25 35
Depth below surface (m)
25
50
75
100
WIL-3
-6 -5 -4
log10Kh (m/s)
Kh for HF interval
Kh for LF interval

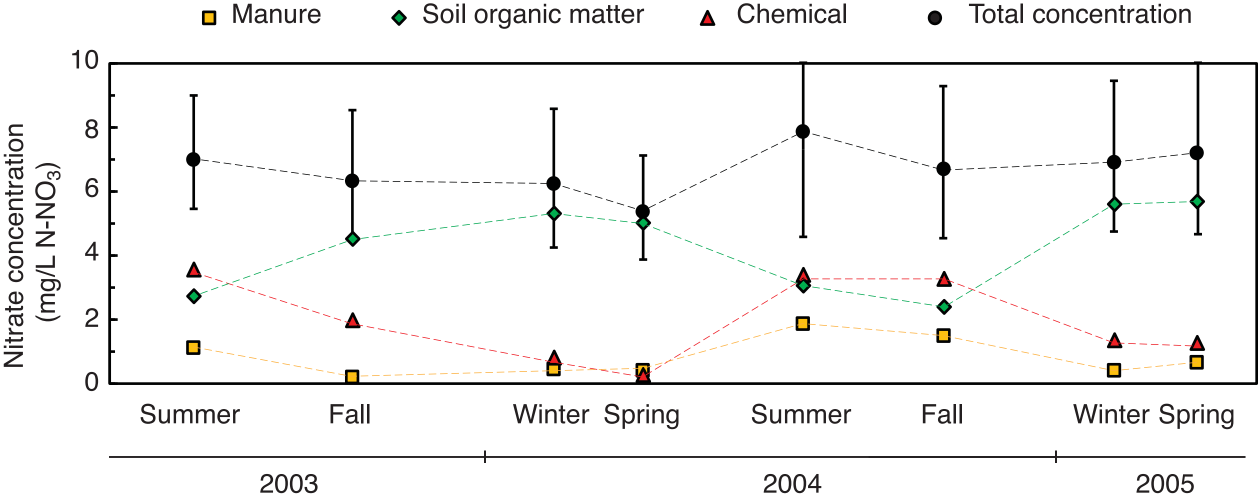

Manure
Soil organic matter
Chemical
Total concentration
Nitrate concentration (mg/L N-NO$_3$)
10
8
6
4
2
0
Summer
Fall
Winter
Spring
Summer
Fall
Winter
Spring
2003
2004
2005

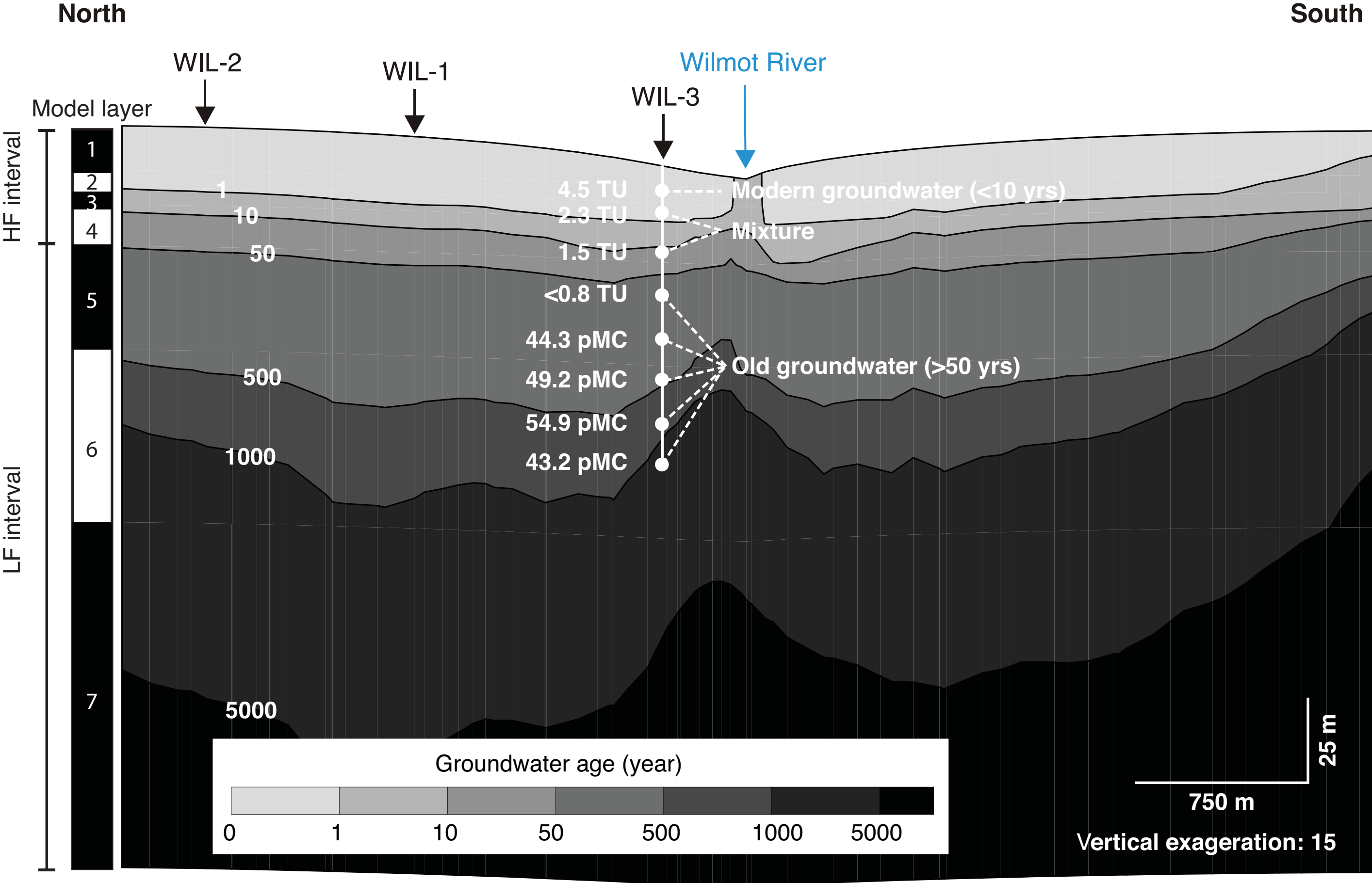
North
South
WIL-2
WIL-1
WIL-3
Wilmot River
Model layer
HF interval
LF interval
1
2
3
4
5
6
7
1
10
50
500
1000
5000
4.5 TU
2.3 TU
1.5 TU
<0.8 TU
44.3 pMC
49.2 pMC
54.9 pMC
43.2 pMC
Modern groundwater (<10 yrs)
Mixture
Old groundwater (>50 yrs)
Groundwater age (year)
0
1
10
50
500
1000
5000
25 m
750 m
Vertical exageration: 15

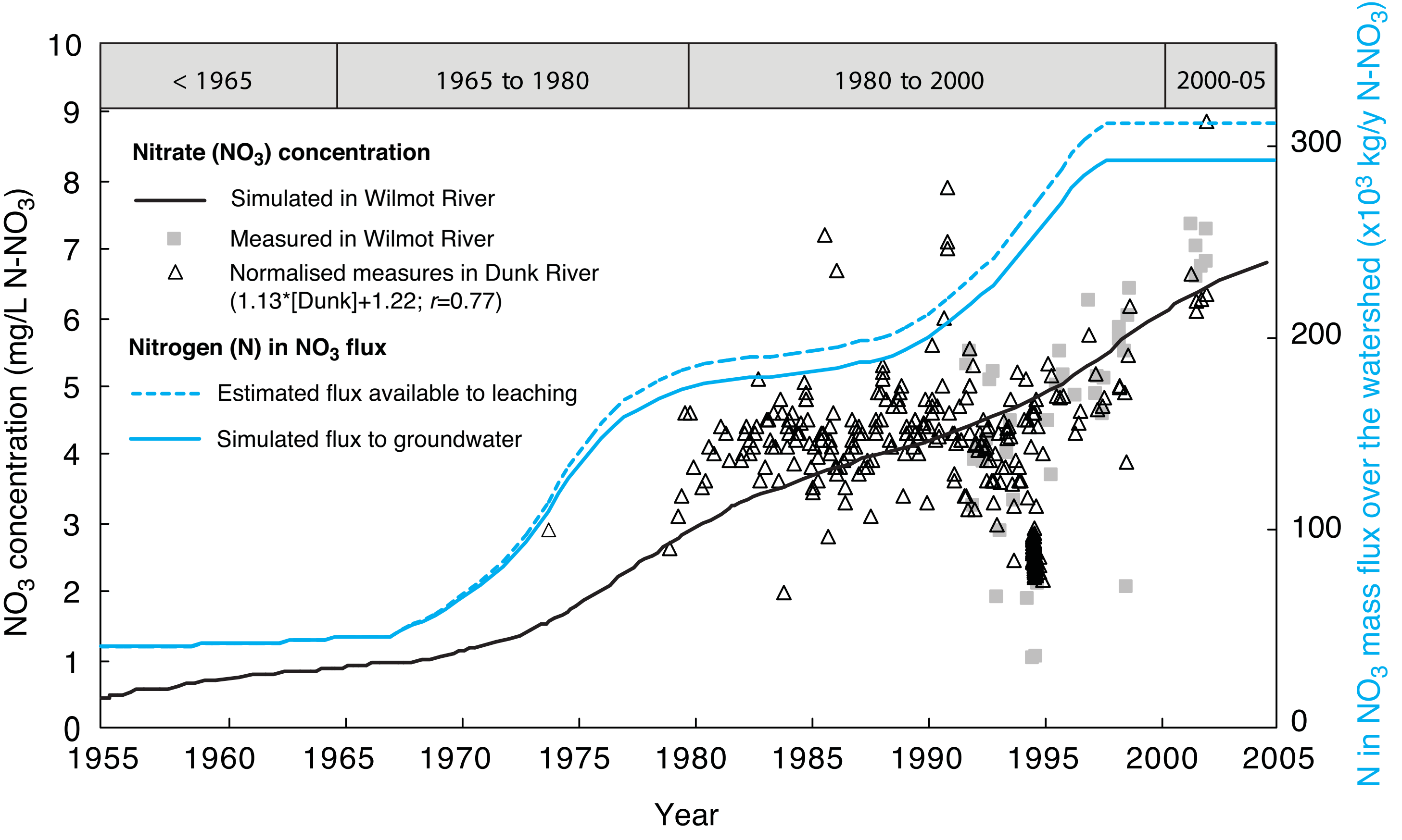

< 1965
1965 to 1980
1980 to 2000
2000-05
Nitrate (NO_3) concentration
Simulated in Wilmot River
Measured in Wilmot River
Normalised measures in Dunk River
(1.13*[Dunk]+1.22; *r*=0.77)
Nitrogen (N) in NO_3 flux
Estimated flux available to leaching
Simulated flux to groundwater
NO_3 concentration (mg/L N-NO_3)
N in NO_3 mass flux over the watershed (x10^3 kg/y N-NO_3)
Year
0
1
2
3
4
5
6
7
8
9
10
0
100
200
300
1955
1960
1965
1970
1975
1980
1985
1990
1995
2000
2005

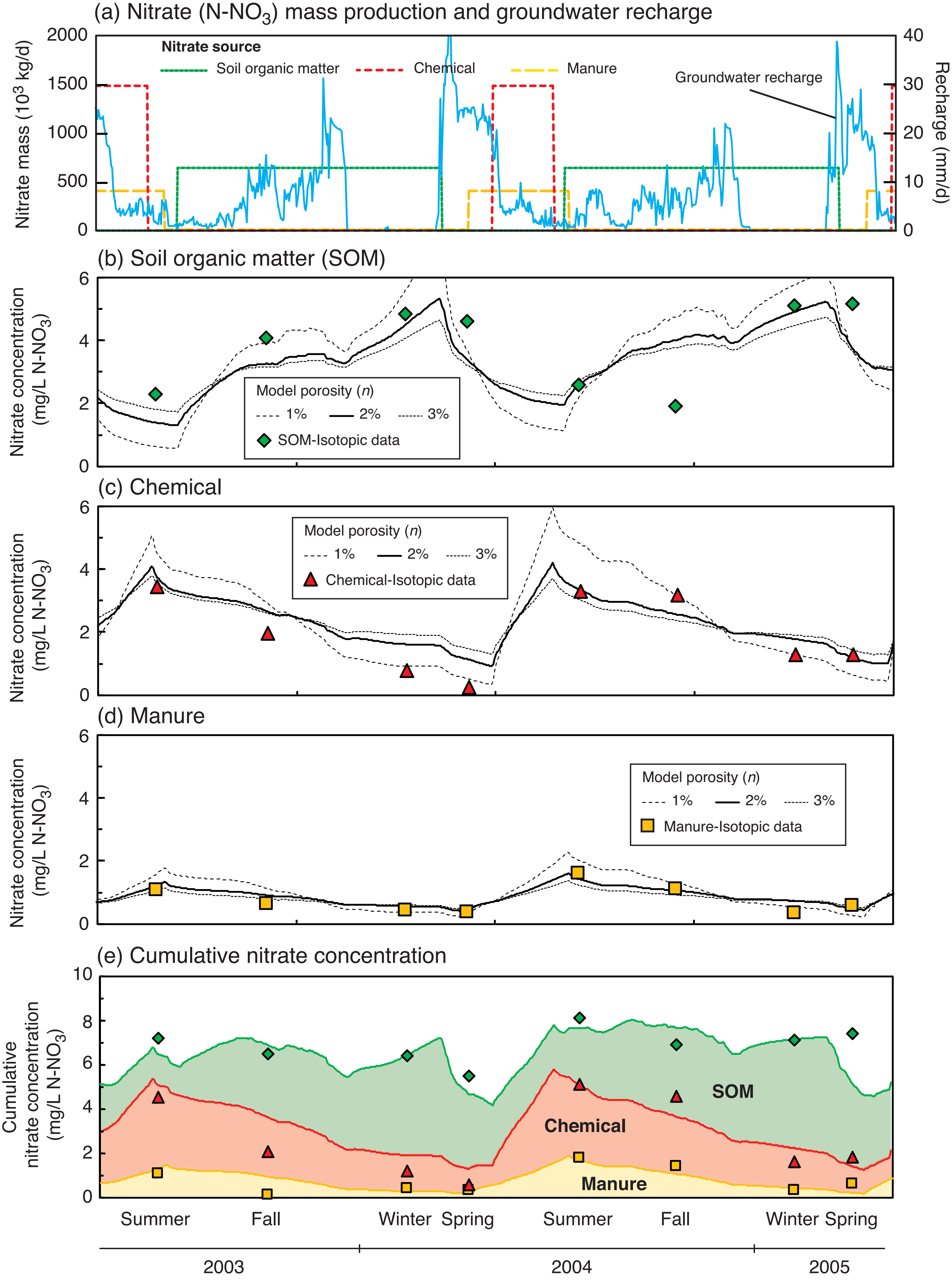

(a) Nitrate (N-NO3) mass production and groundwater recharge
Nitrate source
Soil organic matter
Chemical
Manure
Groundwater recharge
Nitrate mass (10³ kg/d)
Recharge (mm/d)
(b) Soil organic matter (SOM)
Model porosity (n)
1%
2%
3%
SOM-Isotopic data
Nitrate concentration (mg/L N-NO3)
(c) Chemical
Chemical-Isotopic data
(d) Manure
Manure-Isotopic data
(e) Cumulative nitrate concentration
Cumulative nitrate concentration (mg/L N-NO3)
SOM
Chemical
Manure
Summer
Fall
Winter
Spring
2003
2004
2005

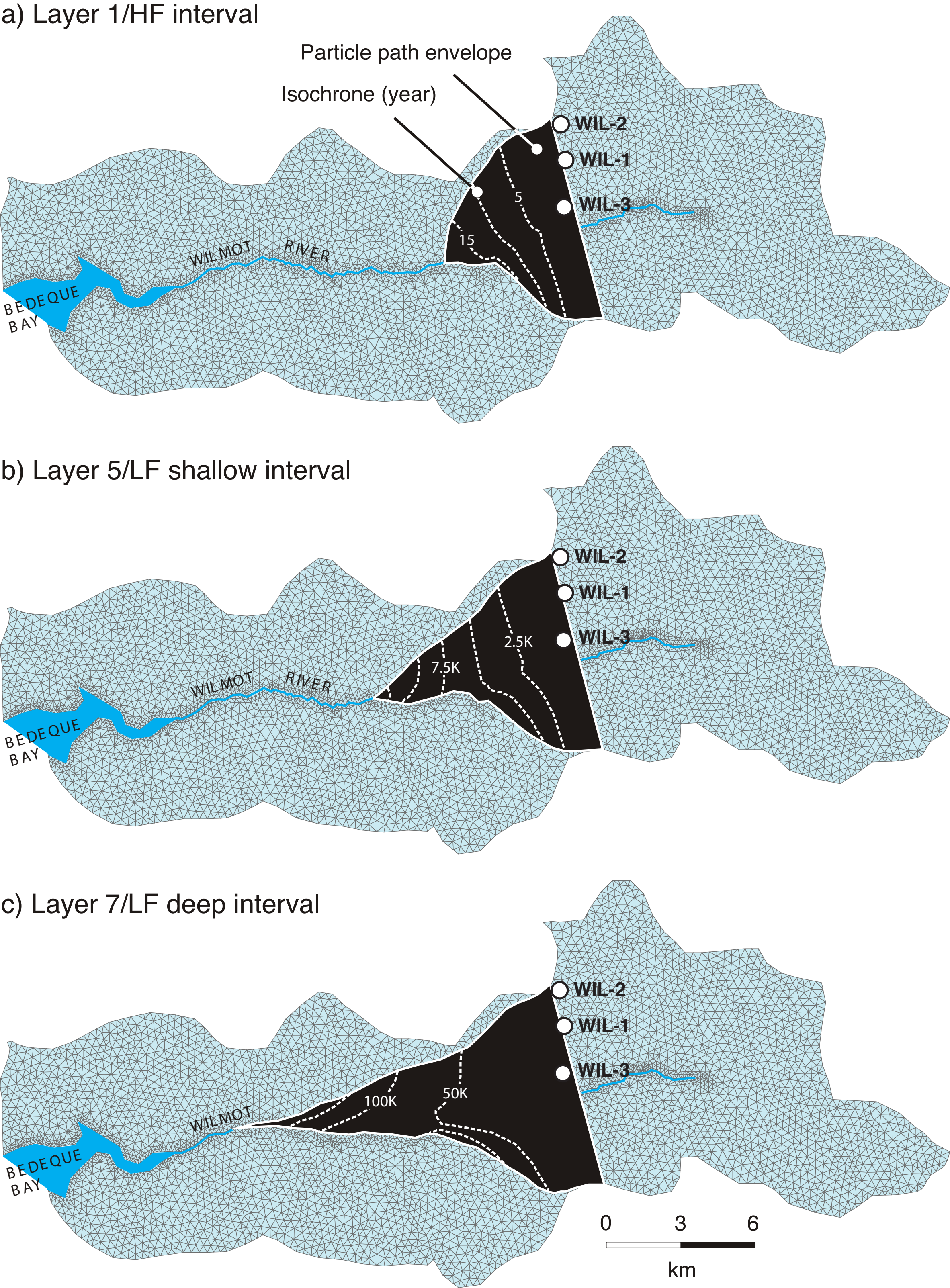
a) Layer 1/HF interval
Particle path envelope
Isochrone (year)
WIL-2
WIL-1
WIL-3
5
15
WILMOT RIVER
BEDEQUE BAY
b) Layer 5/LF shallow interval
WIL-2
WIL-1
WIL-3
2.5K
7.5K
WILMOT RIVER
BEDEQUE BAY
c) Layer 7/LF deep interval
WIL-2
WIL-1
WIL-3
100K
50K
WILMOT
BEDEQUE BAY
0
3
6
km

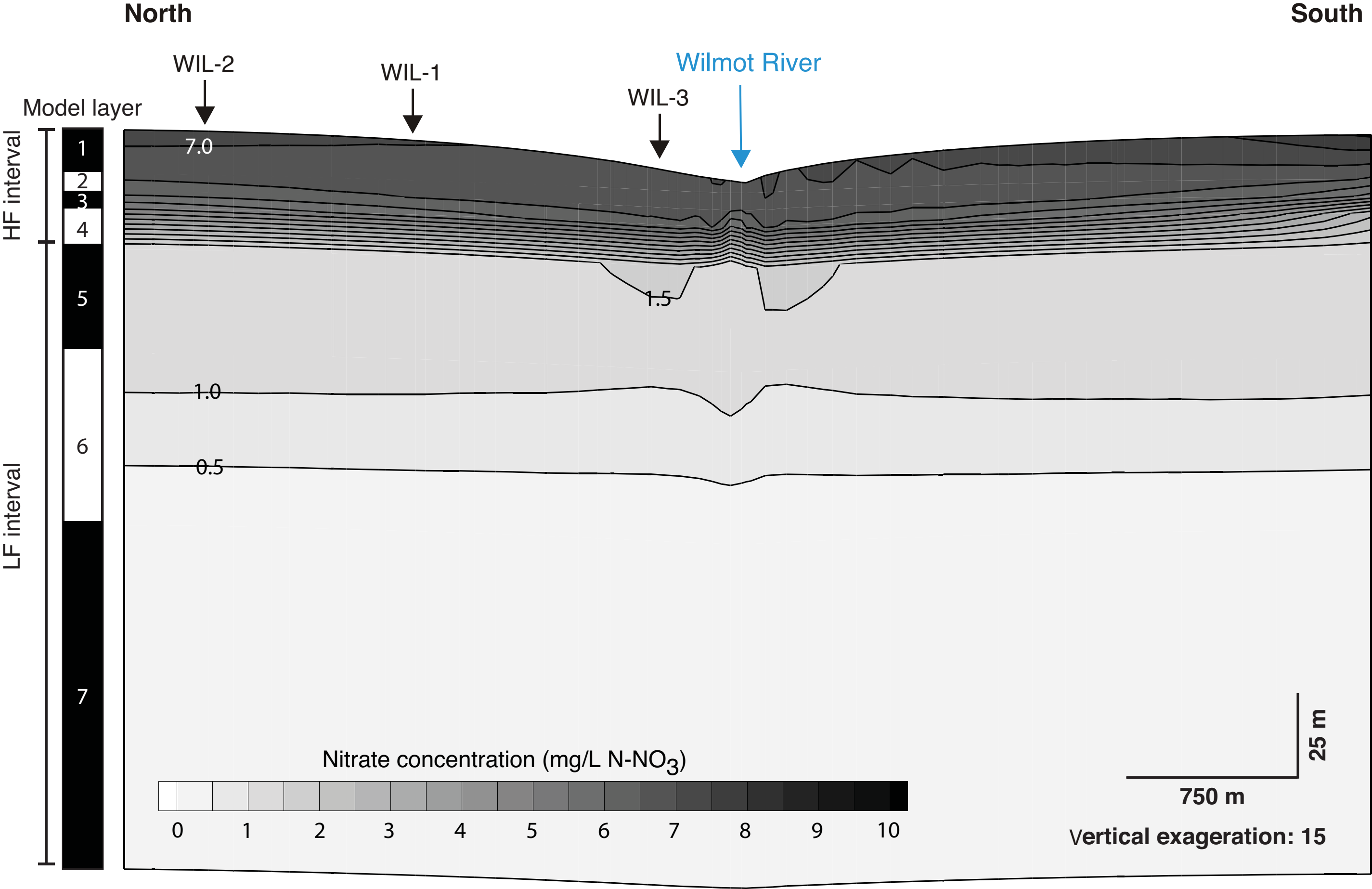

North
South
WIL-2
WIL-1
WIL-3
Wilmot River
Model layer
HF interval
LF interval
1
2
3
4
5
6
7
7.0
1.5
1.0
0.5
Nitrate concentration (mg/L N-NO3)
0
1
2
3
4
5
6
7
8
9
10
25 m
750 m
Vertical exageration: 15

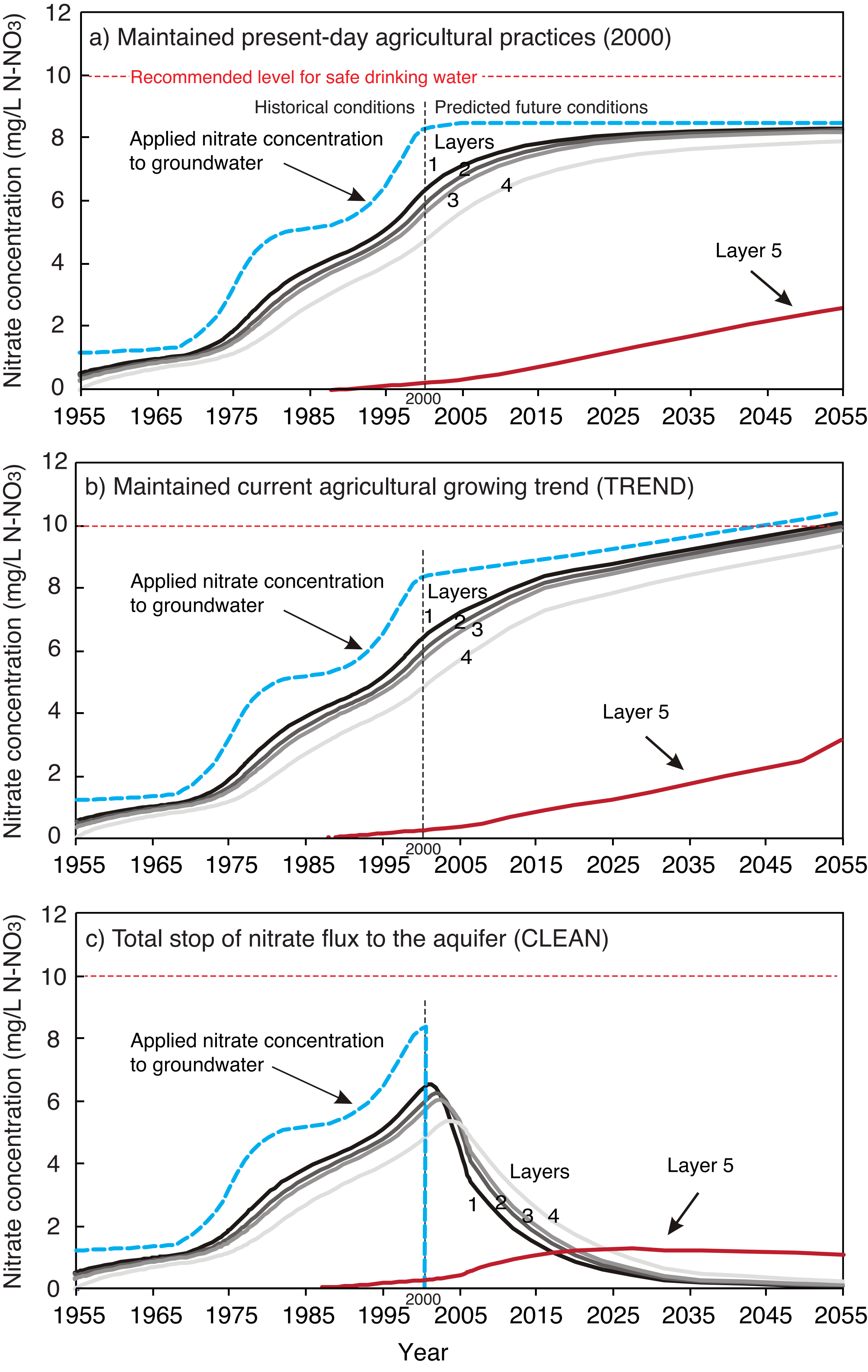
a) Maintained present-day agricultural practices (2000)
Recommended level for safe drinking water
Historical conditions
Predicted future conditions
Applied nitrate concentration to groundwater
Layers
1
2
3
4
Layer 5
b) Maintained current agricultural growing trend (TREND)
Applied nitrate concentration to groundwater
Layers
1
2
3
4
Layer 5
c) Total stop of nitrate flux to the aquifer (CLEAN)
Applied nitrate concentration to groundwater
Layers
1
2
3
4
Layer 5
Nitrate concentration (mg/L N-NO3)
0
2
4
6
8
10
12
1955
1965
1975
1985
1995
2000
2005
2015
2025
2035
2045
2055
Year

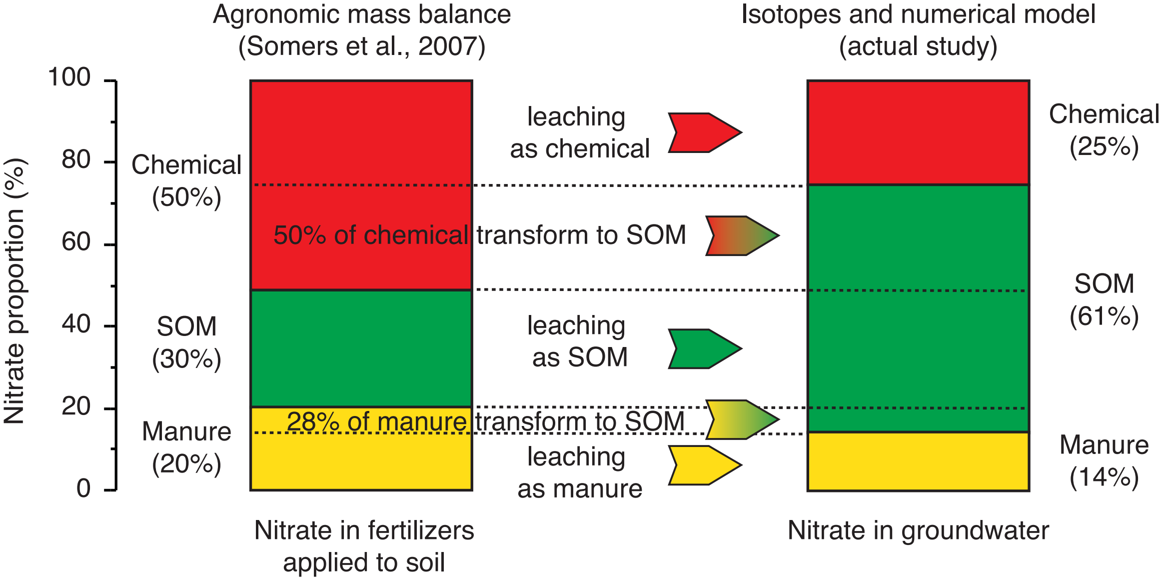

Agronomic mass balance
(Somers et al., 2007)
Isotopes and numerical model
(actual study)
Nitrate proportion (%)
100
80
60
40
20
0
Chemical
(50%)
SOM
(30%)
Manure
(20%)
leaching
as chemical
50% of chemical transform to SOM
leaching
as SOM
28% of manure transform to SOM
leaching
as manure
Chemical
(25%)
SOM
(61%)
Manure
(14%)
Nitrate in fertilizers
applied to soil
Nitrate in groundwater

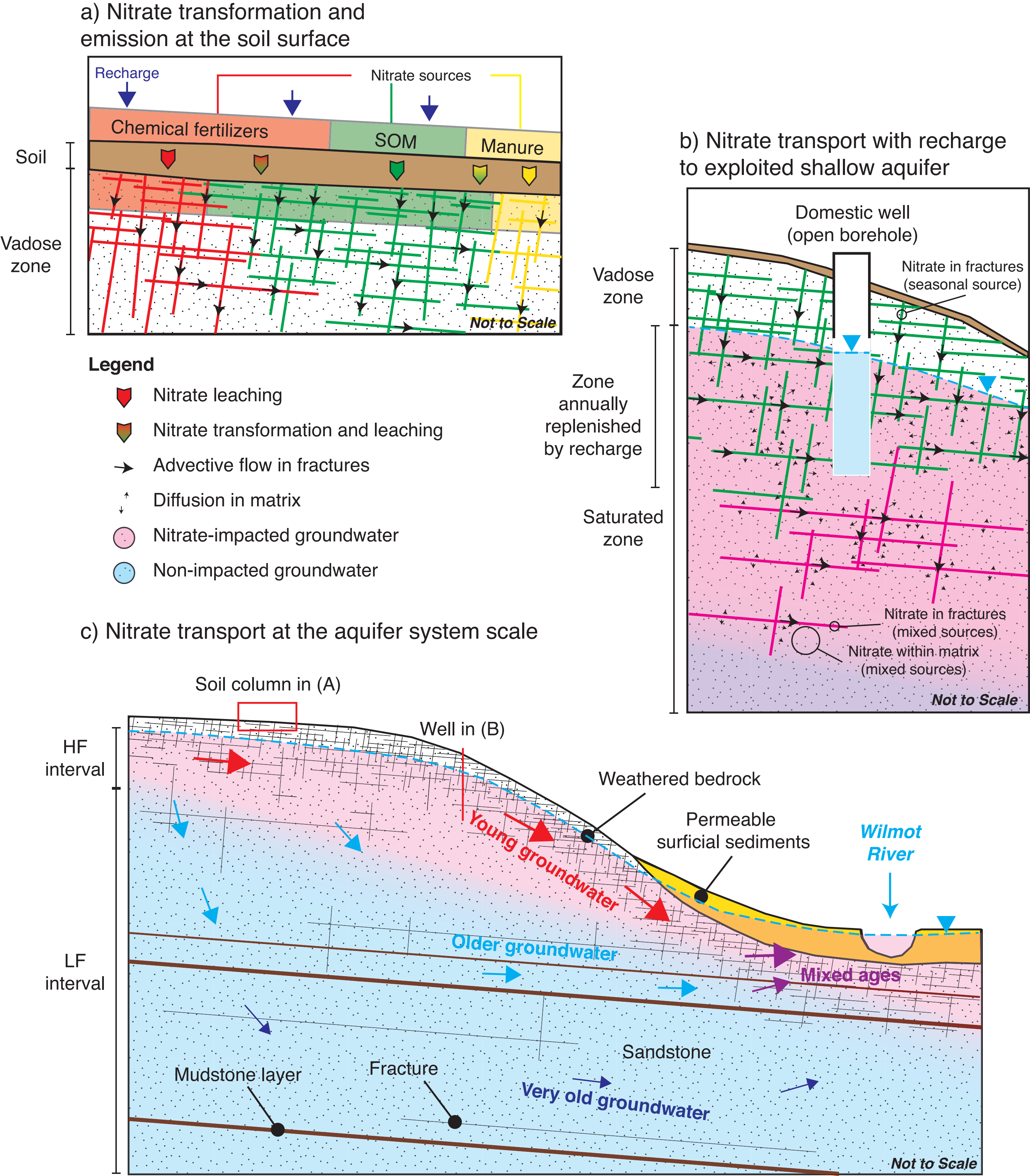

a) Nitrate transformation and emission at the soil surface
Recharge
Nitrate sources
Chemical fertilizers
SOM
Manure
Soil
Vadose zone
Not to Scale
Legend
Nitrate leaching
Nitrate transformation and leaching
Advective flow in fractures
Diffusion in matrix
Nitrate-impacted groundwater
Non-impacted groundwater
b) Nitrate transport with recharge to exploited shallow aquifer
Domestic well (open borehole)
Nitrate in fractures (seasonal source)
Vadose zone
Zone annually replenished by recharge
Saturated zone
Nitrate in fractures (mixed sources)
Nitrate within matrix (mixed sources)
Not to Scale
c) Nitrate transport at the aquifer system scale
Soil column in (A)
Well in (B)
HF interval
LF interval
Weathered bedrock
Permeable surficial sediments
Wilmot River
Young groundwater
Older groundwater
Mixed ages
Sandstone
Mudstone layer
Fracture
Very old groundwater
Not to Scale